

Padé-Summation Approach to QCD β -Function Infrared Properties

F. A. Chishtie,¹ V. Elias,¹ V. A. Miransky,^{1,2,3} T. G. Steele⁴

October 15, 2018

Abstract

In view of the successful asymptotic Padé-approximant predictions for higher-loop terms within QCD and massive scalar field theory, we address whether Padé-summations of the \overline{MS} QCD β -function for a given number of flavours exhibit an infrared-stable fixed point, or alternatively, an infrared attractor of a double valued couplant as noted by Kogan and Shifman for the case of supersymmetric gluodynamics. Below an approximant-dependent flavour threshold ($6 \leq n_f \leq 8$), we find that Padé-summation β -functions incorporating [2|1], [1|2], [2|2], [1|3], and [3|1] approximants whose Maclaurin expansions match known higher-than-one-loop contributions to the β -function series always exhibit a positive pole prior to the occurrence of their first positive zero, precluding any identification of this first positive zero as an infrared-stable fixed point of the β -function. This result is shown to be true regardless of the magnitude of the presently-unknown five-loop β -function contribution explicitly appearing within Padé-summation β -functions incorporating [2|2], [1|3], and [3|1] approximants. Moreover, the pole in question suggests the occurrence of dynamics in which both a strong and an asymptotically-free phase share a common infrared attractor. We briefly discuss the possible relevance of infrared-attractor dynamics to the success of recent calculations of the glueball mass spectra in QCD with $N_c \rightarrow \infty$ via supergravity. As n_f increases above an approximant-dependent flavour threshold, Padé-summation β -functions incorporating [2|2], [1|3], and [3|1] approximants exhibit dynamics controlled by an infrared-stable fixed point over a widening domain of the five-loop \overline{MS} β -function parameter (β_4/β_0). Subsequent to the above-mentioned flavour threshold, all approximants considered exhibit infrared-stable fixed points that decrease in magnitude with increasing flavour number.

1 Introduction

Asymptotic Padé-approximant methods have been utilized to estimate higher order contributions to renormalization-group (RG) functions within both QCD [1, 2, 3] and massive scalar field theory [2, 3, 4], for which such estimates compare quite favourably with explicit calculation [5]. More recently, such methods have been shown to predict RG-accessible coefficients of logarithms within five-loop-order contributions to QCD correlation functions with striking accuracy [6]. These results are all derived from an improvement of Padé-estimated coefficients which incorporates the estimated error of Padé-approximants in predicting the $n!K^{-n}n^\gamma$ asymptotic behaviour expected for n^{th} order coefficients of a field-theoretic perturbative series [7, 8]. For $[N|M]$ approximants, such error is seen to decrease with increasing N and M [1, 2, 7], as well as to favour diagonal and near-diagonal approximants [9].

Of course, the use of such higher approximants becomes tenable only if the corresponding perturbative series is known to sufficiently high order. A known series of the form $\sum_{j=1}^k R_j x^j$ specifies all coefficients within $[N|M]$ -approximants to the series only for $\{N, M\}$ such that $k = N + M$; even four-loop calculations (corresponding to $k = 3$ if the leading x^2 behaviour is factored out from the series) serve only to specify [2|1], [1|2], and [0|3] approximants. Nevertheless, such approximants have been used in conjunction with the anticipated asymptotic error to predict the next (five-loop) coefficient R_4 as well as the corresponding diagonal [2|2] approximant to the full field-theoretic series.[1, 2, 3, 4, 6]

The success of such predictions for those cases in which R_4 is known [1, 3, 6] suggests that

¹Department of Applied Mathematics, The University of Western Ontario, London, Ontario N6A 5B9 CANADA

²Department of Physics, Nagoya University, Nagoya 464-8602 JAPAN

³Permanent Address: Bogolyubov Institute for Theoretical Physics, Ukrainian National Academy of Sciences, UA 252143 Kiev, UKRAINE

⁴Department of Physics & Engineering Physics, University of Saskatchewan, Saskatoon, Saskatchewan S7N 5C6 CANADA

1. Padé approximants determined from $\{R_1, \dots, R_k\}$ more accurately represent the field-theoretic asymptotic series $\sum_{j=0} R_j x^j$ than mere truncation of this series to $\sum_{j=0}^k R_j x^j$;
2. Sufficiently-high Padé-approximants grow arbitrarily close to the function of x represented by the full field-theoretic series, as suggested by asymptotic error formulae [1] following from renormalon-estimates of large- j coefficients in the series [7].

In the absence of alternatives other than explicit series truncation, such “Padé-summation” [1, 2] of the full perturbative series may provide a much wanted means for extrapolating such series to the infrared region. We are particularly interested in two possible scenarios for infrared dynamics within QCD, either the infrared attractor suggested by Kogan and Shifman within the context of supersymmetric gluodynamics [10], or alternatively, dynamics governed by an infrared-stable fixed point. In reference [2], for example, a Padé-summation of the $n_f = 3$ QCD β -function is argued to contain a zero corresponding to an infrared fixed point comparable to that predicted by Mattingly and Stevenson [11, 12].

Indeed it is this claim that provides some of the motivation for our present work. In the approach of ref. [12], an infrared-stable fixed point is argued to occur even when $n_f = 0$, in contradiction to a broadening consensus that values of n_f even larger than 3 are required for infrared-stable fixed points to occur [13, 14, 15, 16, 17]; e.g. $n_f = 8$ is suggested by a two-loop truncation of the QCD β -function, with consequences for the phase-structure of QCD first explored by Banks and Zaks [18].

In the present paper, we utilize the perturbative series for the \overline{MS} QCD β -function, now known in full to four-loop order [19], in order to construct $[N|M]$ Padé summations, which are assumed to provide information about the β -function’s first positive zero or pole (this point is further discussed in Section 2). We are able to extend our analysis past $N + M = 3$ by expressing $N + M = 4$ approximants in terms of the presently-unknown five-loop β function coefficient, which is treated here as a variable parameter. Among the specific issues we address in the sections that follow are:

1. the existence of a flavour-threshold for dynamics governed by an infrared stable-fixed point,
2. whether differing Padé-approximants are consistent in predicting infrared properties of QCD,
3. the dependence of Padé-predictions for β -function infrared properties on the presently-unknown five-loop term,
4. the size of the infrared fixed point, particularly in comparison with the $\alpha_s^* = \pi/4$ benchmark value for chiral-symmetry breaking [13, 14],
5. the existence of a strong phase of QCD for $n_f = 0$ [10] and, possibly, for nonzero n_f as well, and
6. the elevation of the true infrared cutoff (mass gap) of $n_f = 3$ QCD to hadronic mass scales (500 - 700 MeV).

In Section 2, we discuss how Padé-approximants constructed from the known terms of the β -function series can exhibit information about the infrared behaviour of the corresponding couplant. This approach relies upon the Padé-approximant remaining closer to the true β -function than the truncated perturbation series from which the approximant is constructed, as discussed above. We conclude Section 2 by obtaining Padé-summation expressions for QCD \overline{MS} β -functions which incorporate [2|1], [1|2], [2|2], [1|3] and [3|1] approximants to post-one-loop terms in the β -function series. The latter three approximants are expressed in terms of a variable $R_4 (\equiv \beta_4/\beta_0)$ characterizing the presently unknown 5-loop contribution to the \overline{MS} β -function.

In Section 3, we apply such Padé-summation methods to the β -function characterizing $N_c = 3$ QCD with no fundamental fermions. Padé-summation predictions for the infrared structure of $n_f = 0$ QCD in the ‘t Hooft ($N_c \rightarrow \infty$) limit [20] are presented separately in an Appendix. For both cases, we find that no Padé-summation β -function supports the existence of an infrared-stable fixed point for the $n_f = 0$ QCD couplant. Moreover, we demonstrate that the infrared behaviour extracted from Padé- summations of the $n_f = 0$ QCD β -function appears to be governed by an apparent β -function pole, an infrared-attractor of *two* ultraviolet phases of the couplant. This behaviour is in qualitative agreement with that extracted from supersymmetric QCD in the absence of fundamental-representation matter fields [10]. We conclude Section 3 with a brief discussion of the possible applicability of infrared-attractor dynamics to the glueball spectrum for the $N_c \rightarrow \infty$ case.

In Section 4, we extend the analysis of Section 3 to nonzero n_f . Specifically, we examine Padé-summation β -functions which incorporate [2|1], [1|2], [2|2], [1|3] and [3|1] approximants to post-one-loop terms in the perturbative β -function series. We find that all such approximants exhibit a flavour threshold for the occurrence of infrared dynamics characterized by an infrared-stable fixed point. Beneath this threshold, which occurs between 6 and 9 flavours (depending on the approximant), no infrared-stable fixed point is possible *regardless of the magnitude of the unknown five-loop term* (β_4) entering such approximants. Above the threshold, we observe a progressively broadening domain of β_4/β_0 for which an infrared-stable fixed point occurs, as well as a decrease in the magnitude of such fixed points with increasing n_f .

In Section 5, we focus on the infrared behaviour of the $n_f = 3$ case. We show that [2|2], [1|3] and [3|1] Padé-summations of the $n_f = 3$ perturbative β -function series yield similar infrared dynamics to the “gluodynamic” $n_f = 0$ case of Section 3. Such summations are all shown to yield an enhanced mass gap, an infrared boundary to the domain of α_s somewhat in excess of 500 MeV, regardless of the 5-loop contribution to the β -function series. This infrared boundary is shown to be remarkably stable against such 5-loop corrections to the β -function.

2 Methodology

2.1 A Toy β -Function:

Padé-approximants to a function whose Maclaurin series is $1 + \sum_{k=1} R_k x^k$ are well known to be valid for a broader range of the expansion parameter x than truncations of the series. Consider, for example, the following toy β -function

$$\mu^2 \frac{dx}{d\mu^2} = \beta_A(x) \equiv -x^2 [\sec(x) - \tan(x)] \quad (2.1)$$

We have chosen β_A to be asymptotically free, i.e., to have an ultraviolet fixed point at $x = 0$. Since

$$\lim_{x \rightarrow \pi/2} (\sec(x) - \tan(x)) = 0 \quad (2.2)$$

we have also chosen β_A to have an infrared fixed point at $x = \pi/2$. β_A has a subsequent pole at $x = 3\pi/2$, and β_A alternates zeros and poles as x increases by subsequent increments of π . The point here, however, is that the solution to (2.1) will exhibit the same dynamics as depicted in Fig. 1 for x between zero and $\pi/2$, corresponding to a freezing-out of the coupling at the $x = \pi/2$ infrared-stable fixed point.

Suppose, however, that the sum-total of our knowledge of β_A is the first five-terms of this series expansion, corresponding to a hypothetical five-loop β -function calculation:

$$\beta_A^{(5)}(x) = -x^2 \left[1 - x + \frac{x^2}{2} - \frac{x^3}{3} + \frac{5x^4}{24} \right] \quad (2.3)$$

This truncated series is, of course, not equal to zero at the $x = \pi/2$ infrared fixed point. Rather, when $x = \pi/2$, each term in the series is seen to be comparable to prior lower-order terms:

$$\beta_A^{(5)}(\pi/2) = -\frac{\pi^2}{4} [1 - 1.571 + 1.233 - 1.292 + 1.269] \quad (2.4)$$

One would necessarily conclude that the field theoretical calculation leading to (2.3) cannot be extended to large enough x to extract information about the infrared properties of $\beta_A(x)$.

The series (2.3), however, provides sufficient information to construct a [2|2] approximant to the degree-four polynomial within (2.3):

$$\beta_A^{[2|2]}(x) = -x^2 \left[\frac{1 - \frac{x}{2} - \frac{x^2}{12}}{1 + \frac{x}{2} - \frac{x^2}{12}} \right] \quad (2.5)$$

Equation (2.5) is obtained by requiring that the degree-2 numerator and denominator polynomials of the [2|2] approximant be chosen so as to yield a Maclaurin expansion whose first five terms reproduce the five terms in (2.3). One can easily verify that $\beta_A^{[2|2]}$ remains closer to β_A (2.1) over a much larger range of x than $\beta_A^{(5)}$, as given in (2.3). This range is inclusive of the first zero of β_A . $\beta_A^{[2|2]}$ has a positive zero at $x = 1.583$, quite close to β_A 's true

zero at $\pi/2$. Moreover, the denominator in (2.5) remains positive over the entire range $0 \leq x \leq 1.583$, guaranteeing that $x = 1.583$ is infrared-stable (a sign change would render this fixed-point ultraviolet-stable). Thus, Padé-improvement of the information in (2.3) provides a means for extracting information about the infrared properties of β_A that is otherwise inaccessible from the “five-loop” expression.

2.2 β -Function Poles

It should also be noted that (2.5) predicts that a pole at $x = 7.58$ follows the zero at 1.583 without a second intervening zero. This result is qualitatively similar to the true behaviour of β_A , which acquires a pole at $x = 3\pi/2$ subsequent to the zero at $\pi/2$ without any additional intervening zeros. However, accuracy in predicting this pole, as well as any subsequent zeros or poles, is clearly beyond the scope of (2.5), the [2|2] Padé-summation of β_A .

We have seen, however, that Padé methods do provide a window for viewing leading β -function singularities that would otherwise be inaccessible. One cannot automatically dismiss the possibility of such singularities occurring within QCD β -functions. For example, the β -function of $SU(N_c)$ SUSY gluodynamics, which is known *exactly* if no matter fields are present, exhibits precisely such a zero [21]:

$$\beta(x) = -\frac{3N_c x^2}{4} \left[\frac{1}{1 - N_c x/2} \right]; \quad x \equiv \frac{\alpha_s}{\pi}. \quad (2.6)$$

Eq. (2.6), which can be derived via imposition of the Adler-Bardeen theorem upon the supermultiplet of the anomalies [22], implies the existence of a strong ultraviolet phase (the upper branch of Fig. 2) when the couplant x is greater than the β -function pole at $2/N_c$ [10]. Interestingly, the β -function (2.6) is itself a [0|1] approximant once the leading $-3N_c x^2/4$ coefficient is factored out.

To demonstrate how Padé summation provides a window for extracting possible pole singularities in true β -functions, we consider a second toy example

$$\mu^2 \frac{dx}{d\mu^2} \equiv \beta_B(x) = x^2 [\sec(x) + \tan(x)]. \quad (2.7)$$

$\beta_B(x)$ is asymptotically free, but has a positive *pole* at $x = \pi/2$ prior to its first zero at $x = 3\pi/2$. This zero is an *ultraviolet* stable fixed point because of the overall sign change associated with passing through the pole at $x = \pi/2$. The behaviour of $x(\mu)$ for $x < 3\pi/2$ is schematically depicted in Fig 2, with $x = \pi/2$ corresponding to μ_c , the minimum allowed value of μ (assuming the couplant x is real).

Such infrared structure is not at all evident in the “five-loop” approximation to (2.7)

$$\beta_B^{(5)}(x) = -x^2 \left[1 + x + \frac{x^2}{2} + \frac{x^3}{3} + \frac{5x^4}{24} \right], \quad (2.8)$$

an expression which ceases to be close to the true β -function (2.7) for values of x substantially smaller than $x = \pi/2$. However, one can obtain a [2|2] approximant directly from the truncated series in (2.8)

$$\beta_B^{[2|2]}(x) = -x^2 \frac{[1 + \frac{x}{2} - \frac{x^2}{12}]}{[1 - \frac{x}{2} - \frac{x^2}{12}]} \quad (2.9)$$

whose Maclaurin expansion yields (2.8) for its first five terms. The first denominator zero of (2.9) is at $x = 1.583$, in good agreement with the positive pole of (2.7) at $x = \pi/2$. Moreover, the first denominator zero of (2.9) precedes all (positive) numerator zeros, thereby eliminating the possibility of the pole being preceded by an infrared fixed point. Thus, (2.9) and the true β -function (2.7) predict very similar dynamics between the ultraviolet-stable fixed point at $x = 0$ and the infrared-attractor *pole* at $x = \pi/2$. By contrast, the “five-loop” β -function (2.8) can only reproduce the true running couplant in the ultraviolet region where x is near zero.

2.3 Padé-Improvement and Infrared Behaviour

It is to be emphasized that the examples presented above demonstrate how Padé-improvement *may* provide information about the infrared region that a truncated perturbative series cannot. There is no way, of course, to prove that the first positive zero or pole of a given Padé-summation is indeed the first zero or pole of the true β -function.

In the absence of methodological alternatives, however, we will explore below the consequences of *assuming* this to be the case. Corroboration of such an assumption relies ultimately on an explicit comparison of next-order terms calculated for the \overline{MS} QCD β -function series, to Padé-predictions for these terms (*e.g.*, ref [3]). There is reason to be encouraged, however, by the success already demonstrated for Padé predictions of the known five-loop content of the massive scalar field theory β -function [1, 4]. Similar successes are obtained in predicting RG-accessible coefficients within the five loop contributions to QCD vector and scalar fermionic-current correlation functions, as well as within four-loop contributions to the scalar gluonic-current correlation function [3, 6].

The general approach we take is to replace a k -loop truncation of the asymptotic β -function series

$$\beta^{(k)}(x) = -\beta_0 x^2 (1 + R_1 x + \dots R_{k-1} x^{k-1}) \quad (2.10)$$

with an expression incorporating the corresponding $[N|M]$ Padé- approximant ($N + M = k - 1$):

$$\beta^{[N|M]}(x) = -\beta_0 x^2 \left(\frac{1 + a_1 x + \dots + a_N x^N}{1 + b_1 x + \dots + b_M x^M} \right) \quad (2.11)$$

The $N + M$ coefficients $\{a_1, \dots, a_N, b_1, \dots, b_M\}$ are completely determined by the requirement that the first k terms in the Maclaurin expansion of (2.11) replicate $\beta^{(k)}(x)$ (2.10). We then examine $\beta^{[N|M]}$ in order to determine whether or not it is supportive of an infrared-stable fixed point, as in Fig. 1, or an infrared-attractor pole, as in Fig. 2.

If the first positive zero of the degree- N polynomial in the numerator of (2.11) precedes any positive zeros of the degree- M polynomial in the denominator, that first numerator zero corresponds to the infrared-stable fixed point at which the couplant x freezes out in Fig. 1. Alternatively, if the first positive zero in the denominator of (2.11) precedes any positive zeros in the degree- M numerator polynomial, that first denominator zero corresponds to the infrared-attractor pole common to both couplant phases of Fig. 2.

2.4 A Padé Roadmap

It will prove useful to tabulate those formulae required to obtain Padé approximants (2.11) whose Maclaurin expansions reproduce the truncated series (2.10) for the \overline{MS} β -function. Values for β_0 , R_1 , R_2 and R_3 for the β -function, as defined by (2.10), are tabulated in Table 1. Corresponding [2|1] and [1|2] approximants to the truncated series $1 + R_1 x + R_2 x^2 + R_3 x^3$ within (2.10) are given by the following formulae:

n_f	β_0	R_1	R_2	R_3
0	11/4	51/22	2857/352	41.5383
1	31/12	67/31	62365/8928	34.3295
2	29/12	115/58	48241/8352	27.4505
3	9/4	16/9	3863/864	20.9902
4	25/12	77/50	21943/7200	15.0660
5	23/12	29/23	9769/6624	9.83592
6	7/4	13/14	-65/224	5.51849
7	19/12	10/19	-12629/5472	2.42409
8	17/12	1/34	-22853/4896	1.00918
9	5/4	-3/5	-1201/160	1.97366
10	13/12	-37/26	-41351/3744	6.44815
11	11/12	-28/11	-49625/3168	16.3855
12	3/4	-25/6	-6361/288	35.4746
13	7/12	-47/7	-64223/2016	71.6199
14	5/12	-113/10	-70547/1440	145.373
15	1/4	-22	-2823/32	332.091
16	1/12	-151/2	-81245/288	1309.98

Table 1: The known coefficients β_0 and $R_{1,2,3}$ appearing in the QCD β -function (2.10) for $n_f = 0 - 16$, as calculated in [19].

$$\beta^{[2|1]}(x) = -\beta_0 x^2 \left[\frac{1 + a_1 x + a_2 x^2}{1 + b_1 x} \right], \quad (2.12a)$$

$$a_1 = (R_1 R_2 - R_3)/R_2, \quad (2.12b)$$

$$a_2 = (R_2^2 - R_1 R_3)/R_2, \quad (2.12c)$$

$$b_1 = -R_3/R_2, \quad (2.12d)$$

and

$$\beta^{[1|2]}(x) = -\beta_0 x^2 \left[\frac{1 + a_1 x}{1 + b_1 x + b_2 x^2} \right], \quad (2.13a)$$

$$b_1 = (R_3 - R_1 R_2)/(R_1^2 - R_2), \quad (2.13b)$$

$$b_2 = (R_2^2 - R_1 R_3)/(R_1^2 - R_2), \quad (2.13c)$$

$$a_1 = R_1 + b_1. \quad (2.13d)$$

We do not consider the $[0|3]$ -approximant, as this approximant has no possible numerator zeros and therefore cannot lead to an infrared fixed point. The $[3|0]$ -approximant is, of course, the truncated series itself. The “diagonal-straddling” $[1|2]$ and $[2|1]$ approximants are the only $N + M = 3$ approximants for which both infrared-stable fixed points (Fig. 1) and infrared-attractor poles (Fig. 2) are possible, depending on the specific ordering of positive numerator and denominator zeros in (2.12a) and (2.13a). Hence, it is these approximants we will study in subsequent sections.

R_4 , the “next-order” coefficient of the QCD β -function (2.10), is not presently known. Nevertheless, one can construct “diagonal-straddling” $[2|2]$, $[1|3]$ and $[3|1]$ approximants with R_4 taken to be an arbitrary parameter, by utilizing the values for $\{R_1, R_2, R_3\}$ given in Table 1. One finds for the truncated series $\beta^{(5)}(x) = -\beta_0 x^2 [1 + R_1 x + R_2 x^2 + R_3 x^3 + R_4 x^4]$ the following Padé-approximant β -functions:

$$\beta^{[2|2]}(x) = -\beta_0 x^2 \left[\frac{1 + a_1 x + a_2 x^2}{1 + b_1 x + b_2 x^2} \right], \quad (2.14a)$$

$$b_1 = (R_1 R_4 - R_2 R_3)/(R_2^2 - R_1 R_3), \quad (2.14b)$$

$$b_2 = (R_3^2 - R_2 R_4)/(R_2^2 - R_1 R_3), \quad (2.14c)$$

$$a_1 = R_1 + b_1, \quad (2.14d)$$

$$a_2 = R_1 b_1 + b_2 + R_2; \quad (2.14e)$$

$$\beta^{[1|3]}(x) = -\beta_0 x^2 \left[\frac{1 + a_1 x}{1 + b_1 x + b_2 x^2 + b_3 x^3} \right] \quad (2.15a)$$

$$b_1 = \frac{(R_1^2 R_2 - R_2^2 - R_1 R_3 + R_4)}{(2R_1 R_2 - R_1^3 - R_3)}, \quad (2.15b)$$

$$b_2 = \frac{(R_1^2 R_3 - R_1 R_2^2 + R_2 R_3 - R_4 R_1)}{2R_1 R_2 - R_1^3 - R_3}, \quad (2.15c)$$

$$b_3 = \frac{[R_3^2 + R_2^3 - 2R_1 R_2 R_3 + R_4(R_1^2 - R_2)]}{2R_1 R_2 - R_1^3 - R_3} \quad (2.15d)$$

$$a_1 = R_1 + b_1; \quad (2.15e)$$

$$\beta^{[3|1]}(x) = -\beta_0 x^2 \left[\frac{1 + a_1 x + a_2 x^2 + a_3 x^3}{1 + b_1 x} \right], \quad (2.16a)$$

$$a_1 = R_1 - R_4/R_3, \quad (2.16b)$$

$$a_2 = R_2 - R_1 R_4/R_3, \quad (2.16c)$$

$$a_3 = R_3 - R_2 R_4/R_3, \quad (2.16d)$$

$$b_1 = -R_4/R_3. \quad (2.16e)$$

Given the known values of $\{R_1, R_2, R_3\}$ tabulated in Table 1, we have tabulated $\beta^{[2|2]}$'s coefficients $\{a_1, a_2, b_1, b_2\}$ in Table 2 for all n_f -values for which $x = 0$ is an ultraviolet-stable fixed point. These coefficients are all linear in the unknown parameter R_4 . A similar tabulation of the coefficients within $\beta^{[1|3]}$ and $\beta^{[3|1]}$ is presented in Tables 3 and 4, respectively. Because all such Padé-coefficients are R_4 -dependent for a given choice of n_f , one might expect to find infrared stable fixed point behaviour (Fig. 1) for some range of R_4 , infrared-attractor pole behaviour (Fig. 2) for another range of R_4 , and (possibly) some regimes of R_4 for which there are neither numerator nor denominator zeros. Surprisingly, we find in Section 4 that infrared-stable fixed point behaviour as in Fig. 1 does not occur *for any* of the diagonal-straddling approximants (2.12-15) until n_f reaches a threshold value, *regardless of* R_4 . This threshold depends on the approximant considered, but is greater than or equal to 6 for all $[N|M]$ approximants discussed above.

n_f	a_1	a_2	b_1	b_2
0	13.4026-0.0762155 R_4	-22.9153+0.0901663 R_4	-0.0762155 R_4 + 11.0844	0.266848 R_4 - 56.7275
1	116019-0.0850858 R_4	-19.0068+0.0911037 R_4	-0.0850858 R_4 + 9.44058	0.274999 R_4 - 46.3959
2	9.50934-0.0941220 R_4	-15.0709+0.0875660 R_4	-0.0941220 R_4 + 7.52659	0.274187 R_4 - 35.7703
3	7.19456-0.102610 R_4	-11.3292+0.0756438 R_4	-0.102610 R_4 + 5.41678	0.258062 R_4 - 25.4301
4	4.84008-0.110684 R_4	-8.18415+0.0485887 R_4	-0.110684 R_4 + 3.30008	0.219042 R_4 - 16.3139
5	2.67929-0.123291 R_4	-6.19674-0.0112453 R_4	-0.123291 R_4 + 1.41842	0.144208 R_4 - 9.45997
6	0.610851-0.184236 R_4	-6.62748-0.228650 R_4	-0.184236 R_4 - 0.317721	-0.0575739 R_4 - 6.04228
7	1.907466+0.129932 R_4	-0.130346+0.638145 R_4	0.1299318 R_4 + 1.38115	0.569760 R_4 + 1.45066
8	0.245912+0.00135179 R_4	-4.61451+0.214571 R_4	0.00135179 R_4 + 0.216500	0.214531 R_4 + 0.0468084
9	-0.342477-0.0104297 R_4	-7.59305+0.136738 R_4	-0.0104297 R_4 + 0.257228	0.130480 R_4 + 0.0677118
10	-0.880095-0.0108500 R_4	-11.5003+0.099648 R_4	-0.0184997 R_4 + 0.542982	0.0842074 R_4 + 0.317008
11	-1.65139 - 0.00886659 R_4	-17.0050+0.0771335 R_4	-0.00886659 R_4 + 0.894061	0.0545640 R_4 + 0.935218
12	-2.93401-0.00655509 R_4	-25.2430+0.0620604 R_4	-0.00655509 R_4 + 1.23265	0.0347475 R_4 + 1.97982
13	-5.18889-0.00448899 R_4	-38.6692+0.0514389 R_4	-0.00448899 R_4 + 1.52540	0.0212985 R_4 + 3.42939
14	-9.53837-0.00279507 R_4	-63.6700+0.0437023 R_4	-0.00279507 R_4 + 1.76163	0.0121180 R_4 + 5.22737
15	-20.0584-0.00145806 R_4	-123.626+0.0379240 R_4	-0.00145806 R_4 + 1.94165	0.00584673 R_4 + 7.30916
16	-73.4295-0.000423006 R_4	-428.807+0.0335175 R_4	-0.000423006 R_4 + 2.07047	0.00158053 R_4 + 9.61460

Table 2: Coefficients $a_{1,2}$ and $b_{1,2}$ of $\beta^{[2|2]}$, the $[2|2]$ Padé-approximant (2.13) to the QCD β function for $n_f = 0 - 16$. The coefficients are all linear in R_4 , the (presently-) unknown five-loop term in (2.10).

3 Gluodynamics

In this section we consider conventional ($N_c = 3$) QCD with $n_f = 0$. The $N_c \rightarrow \infty$ case is considered separately in an Appendix. This “gluodynamic” limit is of particular interest as a possible projection (without gluinos) of supersymmetric QCD in the absence of fundamental-representation matter fields ($n_f = 0$ SQCD), a theory for which the β -function is known to all orders of perturbation theory [21]. The $n_f = 0$ SQCD β -function (2.6) does not exhibit an infrared-stable fixed point; rather, it exhibits the dynamics of Fig. 2 in which a β -function pole serves as an infrared-attractor, both for a weak asymptotically-free phase, as well as for a strong phase of the now double-valued couplant [10]. Such dynamics differ fundamentally from those of Fig. 1 anticipated from an infrared-stable fixed point, which has been argued elsewhere [12] to occur for QCD even in the $n_f = 0$ gluodynamic limit. Padé-approximant estimates of higher order terms in QCD β -functions [1] and correlators [6] have in fact proven to be most accurate in the $n_f = 0$ case in which “quadratic-Casimir” effects are minimal [1]. Thus, the methodological machinery of the previous section may be particularly well-suited to shed insight on whether the dynamics of Fig. 1 or Fig. 2 characterize QCD’s gluodynamic limit.

For $n_f = 0$, the four-loop \overline{MS} QCD β -function is [19]

$$\beta^{(4)}(x) = -\frac{11}{4}x^2 [1 + 2.31818x + 8.11648x^2 + 41.5383x^3], \quad (3.1)$$

n_f	a_1	b_1	b_2	b_3
0	$9.56239-0.0611053R_4$	$7.24421-0.0611053R_4$	$-24.9099+0.141653R_4$	$-42.5901+0.167582R_4$
1	$8.51104-0.0702708R_4$	$6.34975-0.0702708R_4$	$-20.7090+0.151876R_4$	$-33.9265+0.162617R_4$
2	$7.25658-0.0810329R_4$	$5.27382-0.0810329R_4$	$-16.2327+0.160669R_4$	$-25.7265+0.149477R_4$
3	$5.80845-0.0933552R_4$	$4.03067-0.0933552R_4$	$-11.6367+0.165965R_4$	$-18.3242+0.122349R_4$
4	$4.24716-0.107164R_4$	$2.70716-0.107164R_4$	$-7.21667+0.165032R_4$	$-12.2028+0.07244688R_4$
5	$2.76704-0.123131R_4$	$1.50617-0.123131R_4$	$-3.37387+0.155253R_4$	$-7.80319-0.0141605R_4$
6	$1.72453-0.145814R_4$	$0.795958-0.145814R_4$	$-0.448926+0.135399R_4$	$-4.87066-0.168040R_4$
7	$1.97486-0.200029R_4$	$1.44855-0.200029R_4$	$1.54554+0.105278R_4$	$0.105614-0.517062R_4$
8	$17.0270-0.778954R_4$	$16.9976-0.7789537917R_4$	$4.16776+0.0229104R_4$	$78.2076-3.63659R_4$
9	$-8.58112+0.137934R_4$	$-7.98112+0.137934R_4$	$2.71758+0.0827604R_4$	$-60.2514+1.08502R_4$
10	$-6.27351+0.0358829R_4$	$-4.85044+0.0358829R_4$	$4.14206+0.0510641R_4$	$-54.12482+0.468980R_4$
11	$-6.36697+0.0125229R_4$	$-3.82151+0.0125229R_4$	$5.93697+0.0318765R_4$	$-61.1352+0.277305R_4$
12	$-7.44146+0.00452652R_4$	$-3.27479+0.00452652R_4$	$8.44183+0.0188605R_4$	$-72.6300+0.178562R_4$
13	$-9.70448+0.00151777R_4$	$-2.99019+0.00151777R_4$	$11.7796+0.010191R_4$	$-87.7855+0.116775R_4$
14	$-14.2164+0.000415849R_4$	$-2.91637+0.000415849R_4$	$16.0360+0.00469909R_4$	$-107.043+0.0734726R_4$
15	$-25.0410+7.04348 \cdot 10^{-5} R_4$	$-3.04098+7.04348 \cdot 10^{-5} R_4$	$21.3172+0.00154956R_4$	$-131.384+0.0403041R_4$
16	$-78.8684+2.12019 \cdot 10^{-6} R_4$	$-3.36839+2.12019 \cdot 10^{-6} R_4$	$27.7873+0.000160074R_4$	$-162.269+0.0126837R_4$

Table 3: Coefficients a_1 and $b_{1,2,3}$ of $\beta^{[1|3]}$, the $[1|3]$ Padé-approximant (2.14) to the QCD β -function for $n_f = 0-16$. R_4 is the unknown five-loop contribution to the β -function.

as is evident from substitution of the $n_f = 0$ Table 1 entries into (2.10). This β -function is sufficient to determine the $[1|2]$ - and $[2|1]$ -approximant β -functions via (2.12) and (2.13):

$$\beta^{[2|1]}(x) = -\frac{11}{4}x^2 \left[\frac{1 - 2.7996x - 3.7475x^2}{1 - 5.1178x} \right], \quad (3.2)$$

$$\beta^{[1|2]}(x) = -\frac{11}{4}x^2 \left[\frac{1 - 5.9672x}{1 - 8.2854x + 11.091x^2} \right], \quad (3.3)$$

In both (3.2) and (3.3), the first positive denominator zero (x_d) precedes the first positive numerator zero (x_n). We find from (3.2) that $x_d = 0.195 < x_n = 0.264$, and from (3.3) that $x_d = 0.151 < x_n = 0.168$. As discussed in Section 2, this $0 < x_d < x_n$ ordering of positive zeros is consistent with dynamics in which x_d serves as an infrared attractor for both a strong and a weak asymptotically-free phase (Fig. 2). The first positive numerator zero x_n , if taken seriously, necessarily corresponds to an ultraviolet-stable fixed point because of the β -function sign-change occurring as x passes through x_d .

To test the stability of these conclusions against higher-than-four loop corrections, we add an arbitrary “five-loop” correction to (3.1):

$$\beta^{(5)}(x) = \beta^{(4)}(x) - \frac{11}{4}x^2[R_4x^4]. \quad (3.4)$$

The five-loop β -function (3.4) determines $[2|2]$, $[1|3]$, and $[3|1]$ Padé-approximant β -functions via (2.14), (2.15) and (2.16). These can be read off Tables 2, 3 and 4; we list them explicitly here to facilitate the analysis which follows:

$$\beta^{[2|2]}(x) = -\frac{11}{4}x^2 \left[\frac{1 + (13.403 - 0.076216R_4)x - (22.915 - 0.090166R_4)x^2}{1 + (11.084 - 0.076216R_4)x + (56.728 - 0.26685R_4)x^2} \right] \quad (3.5)$$

$$\beta^{[1|3]}(x) = -\frac{11}{4}x^2 \left[\frac{1 + (9.5624 - 0.061105R_4)x}{1 + (7.2442 - 0.061105R_4)x - (24.910 - 0.14165R_4)x^2 - (42.590 - 0.16758R_4)x^3} \right] \quad (3.6)$$

$$\beta^{[3|1]}(x) = -\frac{11}{4}x^2 \left[\frac{1 + (2.31818 - 0.024074R_4)x + (8.1165 - 0.055808R_4)x^2 + (41.538 - 0.19540R_4)x^3}{1 - 0.024074R_4x} \right] \quad (3.7)$$

Figure 3 exhibits a plot of x_n , the first positive zero of (3.5), and x_d (the first positive denominator zero of (3.5)), as a function of the independent variable R_4 . Such positive zeros are seen to occur for all R_4 . Moreover,

n_f	a_1	a_2	a_3	b_1
0	2.31818-0.0240742 R_4	8.11648-0.0558083 R_4	41.5383-0.195397 R_4	-0.0240742 R_4
1	2.16129-0.0291294 R_4	6.98533-0.0629572 R_4	34.3295-0.203479 R_4	-0.0291294 R_4
2	1.98276-0.0364292 R_4	5.77598-0.0722302 R_4	27.4505-0.210414 R_4	-0.0364292 R_4
3	1.77778-0.0476412 R_4	4.47106-0.0846954 R_4	20.9902-0.213007 R_4	-0.0476412 R_4
4	1.54000-0.0663747 R_4	3.04764-0.102217 R_4	15.0650-0.202286 R_4	-0.0663747 R_4
5	1.26087-0.101668 R_4	1.47479-0.128190 R_4	9.83592-0.149939 R_4	-0.101668 R_4
6	0.928571-0.181209 R_4	-0.290179-0.168265 R_4	5.51849+0.0525830 R_4	-0.181209 R_4
7	0.526316-0.412526 R_4	-2.30793-0.217119 R_4	2.42409+0.952081 R_4	-0.412526 R_4
8	0.0294118-0.990906 R_4	-4.66769-0.0291443 R_4	1.00918+4.62524 R_4	-0.990906 R_4
9	-0.600000-0.506673 R_4	-7.50625+0.304004 R_4	1.97366+3.80322 R_4	-0.506673 R_4
10	-1.42308-0.155083 R_4	-11.0446+0.220695 R_4	6.44815 + 1.71283 R_4	-0.155083 R_4
11	-2.54545-0.0610294 R_4	-15.6645+0.155348 R_4	16.3855+0.955993 R_4	-0.0610294 R_4
12	-4.16667-0.0281892 R_4	-22.0868+0.117455 R_4	35.4746+0.622609 R_4	-0.0281892 R_4
13	-6.71429-0.0139626 R_4	-31.8566+0.0937489 R_4	71.6199+0.444801 R_4	-0.0139626 R_4
14	-11.3000-0.00687884 R_4	-48.9910+0.077730 R_4	145.373+0.337001 R_4	-0.00687884 R_4
15	-22.0000-0.00301122 R_4	-88.2188 + 0.0662468 R_4	332.091+0.265646 R_4	-0.00301122 R_4
16	-75.500-0.000763368 R_4	-282.101+0.0576343 R_4	1309.98 + 0.215347 R_4	-0.000763368 R_4

Table 4: Coefficients $a_{1,2,3}$ and b_1 of $\beta^{[3|1]}$, the $[3|1]$ Padé-approximant (2.15) to the QCD β -function for $n_f = 0 - 16$. R_4 is the unknown five-loop contribution to the β -function.

the first positive denominator zero is seen to precede the first positive numerator zero over the *entire range* of R_4 . This last result confirms that the Fig. 2 dynamics predicted from $[1|2]$ and $[2|1]$ approximants appear to be stable against 5-loop corrections of *arbitrary* magnitude.

These results are corroborated by $\beta^{[1|3]}$ and $\beta^{[3|1]}$. Figure 4 plots the first positive numerator and denominator zeros of (3.6) against R_4 for $\beta^{[1|3]}$, as given by (3.6). A positive numerator zero (x_n) exists only if $R_4 > 150$, whereas at least one positive denominator zero (x_d) occurs for all R_4 . Once again, however, x_d precedes x_n over the entire range of R_4 , suggesting that x_d exists as an infrared-attractor for all values of R_4 . Moreover, the ordering $0 < x_d < x_n$, over all values of R_4 for which x_n exists, precludes any identification of x_n with an infrared-stable fixed point.

Figure 5 plots x_n and x_d against R_4 for $\beta^{[3|1]}$, as given in (3.7). This case is perhaps the most interesting of all, as a positive denominator root x_d is possible only if $R_4 > 0$, as is evident from the denominator of (3.7). Figure 5 shows that x_d continues to precede x_n for all positive values of R_4 . Moreover, when R_4 is negative (and a positive pole x_d is no longer possible), one sees from (3.7) that the numerator polynomial coefficients are all positive-definite, precluding any possibility of positive *numerator* roots. We thus see that an infrared-stable fixed point for $\beta^{[3|1]}$ is unattainable, even for the $R_4 < 0$ region for which no denominator zero occurs at all.

Thus, there does not exist *any* valid $N + M = 4$ approximant ($M > 0$) to the $n_f = 0$ QCD β -function which supports an infrared-stable fixed point, regardless of the magnitude of the presently unknown 5-loop term entering such approximants.¹ Moreover, the Fig. 2 dynamics following from a positive β -function pole preceding any β -function zeros appear to be upheld not only by $[2|1]$ - and $[1|2]$ -approximant β -functions, but also by $[2|2]$ -, $[1|3]$ - and (when $R_4 > 0$) $[3|1]$ -approximant β -functions as well.

One can also utilize asymptotic Padé approximant methods to estimate the magnitude of the infrared attractor (Fig. 2), corresponding to the first positive denominator zero of all the approximants considered so far. An asymptotic error formula [1] enables one to obtain an asymptotic Padé-approximant prediction (APAP) of R_4 from the three preceding terms $\{R_1, R_2, R_3\}$ in the β -function series [3]:²

$$R_4^{APAP} = \frac{R_3^2 [R_2^3 + R_1 R_2 R_3 - 2 R_1^3 R_3]}{R_2 [2 R_2^3 - R_1^3 R_3 - R_1^2 R_2^2]}. \quad (3.8)$$

Utilizing the values $\{R_1, R_2, R_3\}$ listed in Table 1 for $n_f = 0$, one finds from (3.8) that $R_4^{APAP} = 302.2$. If one

¹ $\beta^{[0|4]}$ cannot have a nonzero fixed point, as this approximant has no positive numerator zeros at all. The $M = 0$ case $[\beta^{[4|0]}]$, corresponding to the truncated series itself, exhibits a positive zero identifiable with an infrared fixed point only if $R_4 < 0$, in which case the negative five-loop term must be equal in magnitude to the sum of the preceding (positive) one-through-four-loop terms.

²This formula summarizes the content of the algorithm presented in Sections 2 and 5 of ref. [1]

inserts this value of R_4 into the [2|2]-, [1|3]- and [3|1]-approximant β -functions (3.5), (3.6) and (3.7), one finds reasonable agreement from all three β -functions as to the location of the first positive denominator zero, *i.e.* the infrared-attractor of Fig. 2. This zero is seen to occur at $x_d = 0.11$ for $\beta^{[2|2]}$ and $\beta^{[1|3]}$, and at $x_d = 0.14$ for $\beta^{[3|1]}$, corresponding to values of α_s between 0.35 and 0.44. A similar R_4 -estimate ($R_4 = 270$) can be obtained for the $n_f = 0$ case via the weighted asymptotic Padé approximant procedure (WAPAP) delineated in Section 5 of ref. [1]. This procedure expresses the coefficient $\beta_4 = \beta_0 R_4$ as a degree-4 polynomial in n_f , as would be obtained from an explicit perturbative calculation.³ We reiterate that the $n_f = 0$ case minimizes unknown quadratic Casimir effects and avoids entirely the large uncertainties associated with the cancellation of large n_f -dependent terms within β_4 (as evident from eq. (5.5) of [1]) that characterize $n_f > 0$ estimates based on APAP and WAPAP methods.

We conclude this section by reiterating that the ordering $0 < x_d < x_n$ of positive denominator and numerator zeros of $n_f = 0$ Padé-approximant β -functions suggests the existence of a double-valued couplant (Fig. 2), as already seen in SUSY gluodynamics [10]. Such a scenario is seen to decouple the infrared region ($\mu < \mu_c$) from the domain of purely-perturbative QCD, the domain of (real) α_s . Such a scenario is perhaps also indicative of an additional phase distinguished by strong coupling dynamics at short distances.⁴ Taking the Padé-approximants of the β -function seriously, one concludes that there is an ultraviolet-stable fixed point in that phase. Recall that in SUSY gluodynamics, such a fixed point is at $x = \infty$ [10]. Of course, it is impossible to assert that this ultraviolet-stable fixed point survives in the exact β -function of (non-SUSY) gluodynamics. For example, it may be replaced by an ultraviolet Landau pole.

Regardless of these considerations, the picture with an infrared attractor seems plausible and self-consistent. In such dynamics, both phases may share common infrared properties [10]. The presence of two phases has implications meriting further exploration. Such dynamics are shown in the Appendix to characterize QCD in the $N_c \rightarrow \infty$ limit for all but the aforementioned [3|1]-case with R_4 negative. Indeed, such dynamics may prove pertinent to the unexpected agreement between the glueball mass spectra obtained via lattice methods [23] and those obtained via supergravity wave equations in a black hole geometry [24] following from conjectured duality to large- N_c gauge theories [25], an agreement obtained despite the large bare coupling constant necessarily utilized in the latter approach.

In the section which follows, we extend the analysis of the QCD β -function to nonzero n_f values. We specifically seek to address whether Padé-methods indicate a flavour-threshold for infrared-stable fixed points. However, we also seek insight as to whether there is any evidence for a strong phase of QCD when $n_f > 0$, as such a phase could (conceivably) provide a dynamical mechanism for electroweak symmetry breaking.

4 QCD with Fermions

In this Section, we repeat the analysis of the previous section with $n_f \leq 16$ fermion flavours. The $n_f = 16$ case is the maximum number of flavours consistent with asymptotic freedom: a β -function whose sign is negative as $x \rightarrow 0^+$.

4.1 Four-Loop-Level Results

We first consider the β -function (2.12) incorporating a [2|1] approximant to describe post-one-loop behaviour. This β -function is fully determined by the known two-, three-, and four-loop terms $\{R_1, R_2, R_3\}$ tabulated in Table 1 for $n_f = \{1, 2, \dots, 16\}$. The values of the coefficients $\{a_1, a_2, b_1\}$ characterizing $\beta^{[2|1]}$ in (2.12a) are tabulated in Table 5. Also tabulated in the table are values for x_n , the first positive zero of the numerator $1 + a_1x + a_2x^2$, as well as x_d , the zero of the denominator $1 + b_1x$. Blank entries for x_n, x_d correspond to cases where no positive zero exists. We see from the table that a positive denominator zero precedes the first positive numerator zero for $n_f \leq 5$, in which case that denominator zero serves as an infrared attractor for both a strong and an asymptotically-free ultraviolet phase of the QCD couplant. The denominator zero becomes negative for $n_f \geq 6$; nevertheless, an infrared-stable fixed point (associated with a positive numerator zero) does not occur until $n_f = 7$, as no positive numerator zero exists for $n_f = 6$. The value of $x_n = \alpha_s/\pi$ associated with this infrared-stable fixed point decreases as n_f increases,

³Coefficients β_k listed in [1] must be divided by 4^{k+1} to correspond to our normalization of β -function coefficients: our $\beta(x) = dx/d(\log \mu^2)$ with $x = \alpha/\pi$.

⁴It should be noted here that the presence of an infrared-stable fixed point α^* also implies a possible strong phase of the couplant [14], in addition to the asymptotically-free phase exhibited in Fig. 1. If $\alpha(\mu) > \alpha^*[\mu > 0]$, then α approaches α^* from above as μ approaches zero from above.

as anticipated in other work [13, 14]. If we regard $\alpha_{cr} = \pi/4$ ($x_n = 1/4$) as the threshold value for chiral symmetry breaking [26], we see that the conformal window for QCD is predicted to begin at $n_f = 11$. For $n_f = \{7 - 10\}$, the infrared-stable fixed point x_n is not expected to govern infrared dynamics. Chiral-symmetry breaking should occur before the couplant reaches x_n , and the (now-massive) fermions are expected to decouple from further infrared evolution of α_s [13, 14].

n_f	a_1	a_2	b_1	x_n	x_d
0	-2.79959	-3.74745	-5.11777	0.26394	0.19540
1	-2.75323	-3.63638	-4.91452	0.26820	0.20350
2	-2.76977	-3.64714	-4.75253	0.26710	0.21041
3	-2.91691	-3.87504	-4.69468	0.25586	0.21301
4	-3.40349	-4.56534	-4.94349	0.22557	0.20229
5	-5.40850	-6.93442	-6.66937	0.15435	0.14994
6	19.9461	17.3690	19.01757	—	—
7	1.57664	-1.75513	1.05033	1.3275	—
8	0.245617	-4.66133	0.216205	0.49027	—
9	-0.337065	-7.66401	0.262935	0.33990	—
10	-0.839249	-11.8754	0.583828	0.25699	—
11	-1.49942	-18.3271	1.04603	0.19624	—
12	-2.56052	-28.7791	1.60615	0.14716	—
13	-4.46609	-46.9517	2.24819	0.10593	—
14	-8.33265	-82.5220	2.96735	0.070620	—
15	-18.2356	-171.036	3.76441	0.039903	—
16	-70.8563	-632.698	4.64367	0.012678	—

Table 5: The coefficients a_1 , a_2 and b_1 in $\beta^{[2|1]}$, as given in Eq. (2.12) for $n_f = 0 - 16$. The column x_n tabulates the first positive zero of the numerator. The column x_d tabulates the denominator zero, if positive. For those values of n_f for which real positive numerator (denominator) zeros do not exist, the corresponding entries for x_n (x_d) are left blank. The table shows $0 < x_d < x_n$ for $n_f \leq 5$, corresponding to Fig. 2 type dynamics for this range of n_f . When $n_f \geq 7$, x_n corresponds to an infrared-stable fixed point that decreases as n_f increases.

Qualitatively similar conclusions are obtained from the analysis of $\beta^{[1|2]}$ [eq. (2.13)], although the corresponding values of n_f -thresholds for various infrared properties differ somewhat from those of the [2|1]-approximant case. In Table 6 the values of the constants $\{a_1, b_1, b_2\}$ characterizing $\beta^{[1|2]}$ in (2.13a) are tabulated using the known values for $\{R_1, R_2, R_3\}$ listed in Table 1. When positive, the zero of the numerator $1 + a_1x$ fails to precede positive zeros of the denominator $1 + b_1x + b_2x^2$ until $n_f = 9$ (positive denominator zeros cease occurring after $n_f = 6$, but the numerator zero is negative when $5 \leq n_f \leq 8$). Consequently, $n_f = 9$ is the flavour-threshold for identification of x_n as an infrared-stable fixed point. As before, this fixed point decreases with increasing n_f . Its magnitude does not fall below the $x_n = 1/4$ threshold for chiral-symmetry breakdown until $n_f = 12$, corresponding to a previous prediction [13] of the threshold for QCD's conformal window, consistent with the qualitative picture presented in ref. [14]. Specific predictions for x_n from Tables 5 and 6 agree quantitatively only within this $12 \leq n_f \leq 16$ window. Although the intermediate range of n_f for which $x_n > 1/4$ differs between the two approximants ($7 \leq n_f \leq 10$ for $\beta^{[2|1]}$; $9 \leq n_f \leq 11$ for $\beta^{[1|2]}$), it is nevertheless significant that such a range exists for both cases. In Table 6, a positive denominator zero is seen to precede any positive numerator zeros when $n_f \leq 6$. This behaviour corresponds to the infrared dynamics suggested by Figure 2. Once again, qualitative agreement is seen to occur between the [2|1]- and [1|2]-approximant β -functions insofar as both β -functions predict dynamics governed by a β -function pole x_d for n_f less than some threshold value ($n_f \leq 5$ for $\beta^{[2|1]}$; $n_f \leq 6$ for $\beta^{[1|2]}$).

4.2 Five-Loop Level Results

It is of interest to examine the stability of the qualitative results described above against five-loop corrections to the \overline{MS} β -function, corrections which do not enter our determination of $\beta^{[2|1]}$ and $\beta^{[1|2]}$. As noted in Section 2, Padé-coefficients within $\beta^{[2|2]}$, $\beta^{[1|3]}$ and $\beta^{[3|1]}$ are all seen to be linear in the five-loop β -function correction β_4 ($\beta_4/\beta_0 \equiv R_4$). These coefficients, as defined by equations (2.14a), (2.15a), and (2.16a), are respectively tabulated in Tables 2, 3 and 4. In Table 7 we have tabulated the domain of R_4 for which the first positive numerator zero of the

n_f	a_1	b_1	b_2	x_n	x_d
0	-5.96723	-8.28541	11.0906	0.16758	0.15136
1	-6.14941	-8.31070	10.9765	0.16262	0.15007
2	-6.68998	-8.67274	11.4200	0.14948	0.14177
3	-8.17337	-9.95114	13.2199	0.12235	0.11944
4	-13.8032	-15.3432	20.5809	0.072447	0.072160
5	70.6188	69.3580	-88.9261	—	0.79411
6	5.95098	5.02241	-4.37349	—	1.32141
7	1.93401	1.40769	1.56704	—	—
8	0.274983	0.245571	4.66047	—	—
9	-0.921639	-0.321639	7.31327	1.0850	—
10	-2.13228	-0.709208	10.0353	0.46898	—
11	-3.60614	-1.06069	12.9645	0.27730	—
12	-5.60030	-1.43363	16.1133	0.17856	—
13	-8.56349	-1.84921	19.4406	0.11677	—
14	-13.6105	-2.31052	22.8821	0.073472	—
15	-24.8114	-2.81137	26.3685	0.040304	—
16	-78.8413	-3.34126	29.8352	0.012684	—

Table 6: The coefficients a_1 , b_1 and b_2 in $\beta^{[1|2]}$ as given in Eq. (2.13) for $n_f = 0 - 16$. The column x_d tabulates the first positive denominator zero. The column x_n tabulates the numerator zero, if positive. For those values of n_f for which real positive denominator (numerator) zeros do not exist, the corresponding entries for x_d (x_n) are left blank. The positive denominator zero x_d occurs before any positive numerator zeros for $n_f \leq 6$, suggesting Fig. 2 type dynamics. When $n_f \geq 9$, x_n corresponds to an infrared-stable fixed point that decreases as n_f increases

Padé-approximant β -function precedes any positive denominator zero. Such a numerator zero implies a couplant with Figure 1 type dynamics, in which the numerator zero is an infrared-stable fixed point. We see from Table 7 that such dynamics do not occur at all *regardless of* R_4 unless $n_f \geq 6$. An infrared-stable fixed point cannot occur for $\beta^{[2|2]}$ until $n_f = 7$ (and then only for $R_4 < 0$), nor can it occur for $\beta^{[1|3]}$ until $n_f = 9$. As n_f increases, the domain of R_4 for which Figure 1 type dynamics become possible is seen to broaden for all three Padé-approximant β -functions. The overall picture that emerges is quite similar to that anticipated from Tables 5 and 6. In every case, dynamics governed by an infrared-stable fixed point (Fig. 1) do not occur below a threshold value of n_f , a threshold at or above $n_f = 6$.

Table 8 tabulates the range of R_4 for which a positive pole of $\beta^{[2|2]}$, $\beta^{[1|3]}$ and $\beta^{[3|1]}$ exists and precedes any positive numerator zeros, corresponding to the dynamics schematically presented in Figure 2. For $n_f \leq 5$, $\beta^{[2|2]}$ and $\beta^{[1|3]}$ are seen to exhibit such dynamics regardless of the magnitude of R_4 , the five-loop contribution to the β -function. $\beta^{[3|1]}$ exhibits such Figure 2 type dynamics only if R_4 is positive, as the denominator $1 + b_1 x$ of eq. (2.16a) has a positive zero only if $R_4 > 0$ [$b_1 = -R_4/R_3$]. Such dynamics, however, become impossible for $\beta^{[1|3]}$ and unlikely for $\beta^{[2|2]}$ and $\beta^{[3|1]}$ once n_f gets sufficiently large, as is apparent in Table 8 from the steadily increasing lower bound on R_4 for such dynamics to occur within $\beta^{[2|2]}$ and $\beta^{[3|1]}$.

This large n_f behaviour is illustrated for $n_f = 13$ by plots of the R_4 -dependence of the first positive numerator and denominator zero of $\beta^{[2|2]}$ (Fig. 6), $\beta^{[1|3]}$ (Fig. 7) and $\beta^{[3|1]}$ (Fig. 8). The infrared-stable fixed point associated with the numerator zero in $\beta^{[2|2]}$ and $\beta^{[3|1]}$ is seen to be less than $1/4$ (the assumed threshold for chiral-symmetry breakdown [26]) over the full domain of R_4 indicated in Table 7 for infrared-stable fixed point dynamics, a result is clearly suggestive of $n_f = 13$ being within the conformal window of QCD. The numerator zero in $\beta^{[1|3]}$ is also below $1/4$, as evident from Fig. 7, until the immediate neighbourhood of its singularity at $R_4 = 6394$.

The decrease of the infrared fixed point with increasing n_f is also common to all Padé-approximant β -functions. This behaviour, as already seen in Tables 5 and 6 for $\beta^{[2|1]}$ and $\beta^{[1|2]}$, is illustrated for $\beta^{[2|2]}$ in Fig. 9, in which the magnitudes of x_n are displayed as functions of R_4 for $n_f = \{9 - 16\}$. Such results are consistent with the phase structure anticipated in ref. [14], as already noted. It is also worth mentioning that the general picture we obtain, particularly the need for a critical number of flavours for an infrared-stable fixed point to occur at all, agrees surprisingly well with a lattice study [27].

n_f	[2 2]	[1 3]	[3 1]
0	No R_4	No R_4	No R_4
1	No R_4	No R_4	No R_4
2	No R_4	No R_4	No R_4
3	No R_4	No R_4	No R_4
4	No R_4	No R_4	No R_4
5	No R_4	No R_4	No R_4
6	No R_4	No R_4	$R_4 < -105$
7	$R_4 < 0.21$	No R_4	$R_4 < -2.1$
8	$R_4 < 21.6$	No R_4	$R_4 < 1.2$
9	$R_4 < 57.2$	$R_4 < 62.3$	$R_4 < 3.6$
10	$R_4 < 128.4$	$R_4 < 174.9$	$R_4 < 12.9$
11	$R_4 < 274.6$	$R_4 < 508.5$	$R_4 < 38.4$
12	$R_4 < 594.9$	$R_4 < 1644$	$R_4 < 110$
13	$R_4 < 1384$	$R_4 < 6394$	$R_4 < 340.3$
14	$R_4 < 3750$	$R_4 < 34187$	$R_4 < 1226$
15	$R_4 < 14262$	$R_4 < 355521$	$R_4 < 6057$
16	$R_4 < 174589$	$R_4 < 37198800$	$R_4 < 92883$

Table 7: The domain of R_4 for which an infrared fixed point occurs for $\beta^{[2|2]}$, $\beta^{[1|3]}$ and $\beta^{[3|1]}$. The ranges of R_4 listed (for a given choice of n_f) are those for which a positive numerator zero exists and precedes any positive denominator zeros of the Padé-approximant β -function.

5 QCD's Infrared Boundary

The case of three flavours is of obvious interest, as Padé-extrapolations to the infrared region can be compared to the known empirical dynamics at the onset of the infrared region. We know, for example, that evolution of the running coupling constant from its well-determined value at $\mu = M_z$ [28] leads to a prediction [3]

$$\alpha_s(n_f = 3; \mu = 1 \text{ GeV}) = 0.48 \begin{matrix} +0.09 \\ -0.07 \end{matrix} \quad (5.1)$$

We also know that QCD *as a theory of quarks and gluons* ceases to exist at momentum scales approaching Λ_{QCD} , although the interpretation of Λ_{QCD} is subject to redefinition for each successive order of perturbation theory.

Tables 5-7 show quite clearly that an infrared-stable fixed point for $n_f = 3$ QCD is unsupported by all Padé-approximant β -functions considered here, regardless of the magnitude of R_4 . This result contradicts the infrared-stable fixed point obtained from the analysis of a lower-order expression for the β -function in refs. [11] and [12], although the absence of such a fixed point at $n_f = 3$ is supported by more recent work [17]. We also note that *all* Padé-approximant β -functions considered here exhibit Figure 2 type dynamics, regardless of R_4 , except for $\beta^{[3|1]}$ when $R_4 < 0$. In such dynamics, the β -function pole x_d occurs at momentum-scale μ_c . As evident from Fig. 2, the infrared region $\mu < \mu_c$ is inaccessible to the (real) couplant $x(\mu)$, suggesting that μ_c fulfills the infrared cutoff role commonly ascribed to Λ_{QCD} , the “Landau pole” obtained through use of the truncated β -function series.

In Figs. 10-12, we have exhibited the R_4 dependence of the β -function pole x_d for $\beta^{[2|2]}$, $\beta^{[1|3]}$ and $\beta^{[3|1]}$ when $n_f = 3$. The first positive numerator zero is also displayed in all three figures, and is seen to be larger than x_d for all R_4 values considered. We note from Figs. 10 and 11 the apparent stability of x_d in $\beta^{[2|2]}$ and $\beta^{[1|3]}$ against changes in R_4 when R_4 is negative. Both figures indicate an infrared-attractor near $x_d = 0.4$ ($\alpha_s \cong 1.3$), a value well-above the anticipated threshold for chiral-symmetry breaking.

Given knowledge of an initial value, one can utilize Padé approximant β -functions to estimate the infrared cutoff μ_c . To demonstrate this, we assume from the central value of (5.1) that $x(1 \text{ GeV}) = \alpha_s(1 \text{ GeV})/\pi = 0.153$. The equation

$$\mu^2 \frac{dx}{d\mu^2} = \beta^{[N|M]}(x) \quad (5.2)$$

can be inverted to determine μ_c the value of μ corresponding to the first positive pole of $\beta^{[N|M]}$, Figure 2's infrared

n_f	[2 2]	[1 3]	[3 1]
0	All R_4	All R_4	$R_4 > 0$
1	All R_4	All R_4	$R_4 > 0$
2	All R_4	All R_4	$R_4 > 0$
3	All R_4	All R_4	$R_4 > 0$
4	All R_4	All R_4	$R_4 > 0$
5	All R_4	All R_4	$R_4 > 0$
6	$R_4 > -105$	$R_4 > -35.4$	$R_4 > 0$
7	No R_4	$R_4 > 0.2$	$R_4 > 0$
8	No R_4	$R_4 > 21.5$	$R_4 > 1.2$
9	$R_4 > 4848$	No R_4	$R_4 > 3.6$
10	$R_4 > 2964$	No R_4	$R_4 > 12.9$
11	$R_4 > 2990$	No R_4	$R_4 > 38.4$
12	$R_4 > 3652$	No R_4	$R_4 > 110$
13	$R_4 > 5020$	No R_4	$R_4 > 340.3$
14	$R_4 > 7759$	No R_4	$R_4 > 1226$
15	$R_4 > 14491$	No R_4	$R_4 > 6057$
16	$R_4 > 174589$	No R_4	$R_4 > 92883$

Table 8: The domain of R_4 for which a positive denominator zero exists and precedes any positive numerator zeros of $\beta^{[2|2]}$, $\beta^{[1|3]}$ and $\beta^{[3|1]}$, respectively. Such a condition corresponds to the Figure 2 scenario for coupling constant evolution, in which the positive denominator zero is an infrared attractor for both a strong and weak phase of the couplant.

attractor $x_d = x(\mu_c)$:

$$\mu_c(\text{GeV}) = \exp \left[\frac{1}{2} \int_{x(1\text{GeV})}^{x_d} \frac{dx'}{\beta^{[N|M]}(x')} \right] \quad (5.3)$$

We have utilized (5.3) to plot predicted values of μ_c for [2|2]; [1|3]; and [3|1]-approximant β -functions against the unknown 5-loop β -function coefficient $R_4 (\equiv \beta_4/\beta_0)$. Fig. 13 utilizes $\beta^{[2|2]}$, as determined by the $n_f = 3$ row of Table 2, to predict μ_c , given $x(1) = 0.153$. The curve terminates with $\mu_c = 1 \text{ GeV}$ at $R_4 = 128$, since x_d (the infrared attractor) is itself equal to 0.153 at this value of R_4 . What is noteworthy, however, is the stability of μ_c over the entire range of negative R_4 . Fig. 13 is clearly indicative of QCD's infrared cutoff (mass gap) occurring not much below the ρ mass: $\mu_c \rightarrow 660 \text{ MeV}$ as $R_4 \rightarrow -\infty$.

Thus Fig. 13 is indicative of a lower bound for μ_c well-above the phenomenological value for Λ_{QCD} when $n_f = 3$. The bound on μ_c obtained from $\beta^{[2|2]}$ remains well above Λ_{QCD} even if the estimate for $\alpha_s(1 \text{ GeV})$ is reduced to the floor of its empirical range. Fig. 14 utilizes $\beta^{[2|2]}$ in conjunction with the lower-bound value of (5.1) for $\alpha_s(1 \text{ GeV})$ [$x(1) = \alpha_s(1 \text{ GeV})/\pi = 0.1305$]. The figure continues to predict insensitivity to R_4 over the entire negative range of R_4 , with a somewhat diminished lower bound on μ_c : $\mu_c \rightarrow 550 \text{ MeV}$ from above as $R_4 \rightarrow -\infty$.

The behaviour described above is virtually identical to that obtained by utilizing $\beta^{[1|3]}$ within (5.3). Figures 13 and 14 display μ_c as a function of R_4 , with $x(1) = 0.153$ [Fig 15] and $x(1) = 0.1305$ [Fig 16]. The expression for $\beta^{[1|3]}$ utilized in the integrand of (5.3) can be extracted from the $n_f = 3$ row of Table 3. Both curves terminate at $\mu_c = 1 \text{ GeV}$ at R_4 values corresponding to the infrared attractor x_d being equal to $x(1 \text{ GeV})$ [$x_d = 0.153$ and $x_d = 0.1305$, respectively]. Both curves also demonstrate the same stability of μ_c against changes in R_4 , as well as virtually the same lower bounds for μ_c as obtained in Figs. 13 and 14 from $\beta^{[2|2]}$.

As noted earlier, an infrared attractor associated with an $n_f = 3$ β -function pole occurs within $\beta^{[3|1]}$ only for $R_4 > 0$. In Fig. 17, we plot the $\beta^{[3|1]}$ -prediction for the value of μ_c , as obtained from (5.3), against positive values of R_4 . Using the central value $x(1) = 0.153$ from (4.1), we see that $\mu_c > 600 \text{ MeV}$ over the entire (positive) range of R_4 .

For $R_4 < 0$, $\beta^{[3|1]}(x)$ no longer has a pole. This does not mean, however, that $\alpha_s(\mu)$ has a domain in which μ can get arbitrarily close to zero. Rather, when $R_4 < 0$, there will exist a Landau pole, *i.e.* a minimum value of μ at which α_s will diverge:

$$\mu_L = \exp \left(\frac{1}{2} \int_{x(1\text{GeV})}^{\infty} \frac{dx}{\beta^{[3|1]}} \right) \quad (5.4)$$

Similar dynamics characterize the evolution of $\alpha_s(\mu)$ that follows from the one-loop β -function [$\beta(x) = -\beta_0 x^2$], even though this β -function itself has neither poles nor non-zero fixed points. We have utilized (5.4) in Fig. 18 to find the minimum value of μ as a function of R_4 . If $x(1 \text{ GeV}) = 0.153$, consistent with (5.1), we then find that μ_L approaches 530 MeV from above as $R_4 \rightarrow -\infty$.

In *every* case we consider, it is clear that the domain of $\alpha_s(\mu)$ when $n_f = 3$ is bounded from below by hadronic mass scales comparable to or somewhat below the ρ -mass. Padé-approximant β -functions appear to decouple the infrared region from α_s at values of μ substantially larger than Λ_{QCD} .

6 Conclusions

Utilizing Padé-summation QCD β -functions whose Maclaurin expansions reproduce the known terms of the \overline{MS} β -function series, we obtain a surprising degree of agreement with infrared properties predicted [13, 14, 17] via the 't Hooft renormalization scheme [29] in which the β -function is truncated subsequent to two-loop order. Within the context of $N_c = 3$ QCD, we find clear evidence for a flavour-threshold between $n_f = 6$ and $n_f = 9$ for any possibility at all of infrared dynamics governed by an infrared-stable fixed point. For $n_f < 6$, no approximant-based β -function (other than the truncated series itself) is able to yield a positive zero that is not preceded by a positive pole, regardless of the as-yet-unknown magnitude of the five-loop contribution (R_4) to the \overline{MS} β -function series (2.10). We reiterate that such a zero can be identified as an infrared-stable fixed point only if it is *not* preceded by a positive β -function pole.

We also find (Section 4) that when n_f exceeds the (approximant-dependent) flavour threshold for possible infrared-stable fixed-point dynamics, the magnitude of that fixed point is seen to decrease as n_f increases (Tables 5 and 6 and Figure 9). The true conformal window of QCD is not expected to begin until the infrared-stable fixed point is sufficiently small to preclude chiral-symmetry breaking in the infrared region [13, 14]. In Section 4, we corroborate this window's onset at 11-13 flavours, as anticipated from two-loop results [13, 14].

For values of n_f below the (approximant-dependent) threshold for a possible infrared-stable fixed point, Padé-summations of the \overline{MS} β -function are indicative of infrared dynamics governed by a β -function pole, as has already been observed for N=1 SQCD in the absence of fundamental-representation matter fields [10]. Such a positive pole preceding all positive zeros of the β -function is found to occur for $n_f \leq 5$ for all Padé-approximant β -functions constructed from the \overline{MS} β -function series, regardless of the unknown five-loop term (R_4) in that series, except for the β -function incorporating both a [3|1]-approximant to higher-loop effects and a negative value of R_4 . Infrared dynamics governed by such a pole have a number of phenomenologically interesting properties. Salient among these is the occurrence of an infrared cut-off μ_c on the domain of the QCD couplant $\alpha_s(\mu)/\pi$ (Figure 2). We find (Figs. 13-17) the magnitude of μ_c to be quite stable against changes in R_4 , and to be bounded from below by values larger than Λ_{QCD} and comparable to low-lying meson masses (500-700 MeV). Such an infrared boundary occurs even for the [3|1]-approximant case with $R_4 < 0$, a case for which a positive β -function pole does not exist. For this case the infrared boundary corresponds to a Landau pole at similar hadronic mass scales (Fig. 18).

Pole-dominated infrared dynamics have also been argued [10] to imply the existence of a strong phase that devolves to the same infrared attractor as the asymptotically-free phase of the QCD couplant. In such dynamics, both phases may share common infrared properties [10]. As we have noted at the end of Section 3, such dynamics may provide a clue as to why lattice results for the glueball spectrum appear to be in agreement with results obtained in the strong-coupling, large- N_c limit of $SU(N_c)$ via supergravity wave equations within a black hole geometry.

Acknowledgments

V.E. and T.G.S. are grateful for support from the Natural Sciences and Engineering Research Council of Canada. V.A.M. is grateful to Koichi Yamawaki for his warm hospitality at Nagoya University, where this paper was finished. The work of V.A.M. was supported by the Grant-in-Aid of the Japan Society for the Promotion of Science No. 11695030.

Appendix: Gluodynamics in the 't Hooft Limit

If the product of N_c and α_s is finite and nonzero in the $N_c \rightarrow \infty$ limit, the $n_f = 0$ \overline{MS} $SU(N_c)$ β -function in this same limit is given by [19]

$$\mu^2 \frac{d\lambda}{d\mu^2} = -\frac{11}{3}\lambda^2 [1 + R_1\lambda + R_2\lambda^2 + R_3\lambda^3 (+ R_4\lambda^4 \dots)] \quad (\text{A.1a})$$

$$\lambda \equiv N_c \alpha_s(\mu)/4\pi, \quad (\text{A.1b})$$

$$R_1 = 34/11, \quad (\text{A.1c})$$

$$R_2 = 2857/198, \quad (\text{A.1d})$$

$$R_3 = 86.04326. \quad (\text{A.1e})$$

The coefficients subsequent to R_3 in (A.1a) remain unknown at present. However, the known coefficients in (A.1a) are sufficient to determine Padé-summation functions incorporating [2|1] and [1|2] approximants via (2.12) and (2.13):

$$\beta^{[2|1]}(\lambda) = -\frac{11}{3}\lambda^2 \frac{[1 - 2.87219\lambda - 4.00209\lambda^2]}{[1 - 5.96310\lambda]} \quad (\text{A.2})$$

$$\beta^{[1|2]}(\lambda) = -\frac{11}{3}\lambda^2 \frac{[1 - 5.40935\lambda]}{[1 - 8.50026\lambda + 11.8442\lambda^2]}. \quad (\text{A.3})$$

In both of these approximations, the first positive zero of the denominator [0.1677 in (A.2) and 0.1483 in (A.3)] precedes the first positive zero of the numerator [0.2595 in (A.2) and 0.1849 in (A.3)], excluding Figure 1 type infrared-stable fixed point dynamics. Rather, both approximations support Figure 2 type dynamics, in which the first positive denominator zero (λ_d) serves as an infrared attractor for both a weak and a strong ultraviolet phase.

Such behaviour suggests that both phases may share common infrared properties, as the running couplants in both phases evolve towards the same infrared attractor. This behaviour is corroborated by [1|3] and [2|2] Padé-summation β -functions whose Maclaurin expansions reproduce (A.1a) inclusive of an arbitrary five-loop contribution R_4 . For example, we find from comparison of (2.15) to (A.1a) that

$$\beta^{[1|3]}(\lambda) = -\frac{11}{3}\lambda^2 \left[\frac{1 + a_1\lambda}{1 + b_1\lambda + b_2\lambda^2 + b_3\lambda^3} \right]; \quad (\text{A.4a})$$

$$a_1 = 15.8424 - 0.0379166R_4, \quad (\text{A.4b})$$

$$b_1 = 12.7515 - 0.0379166R_4, \quad (\text{A.4c})$$

$$b_2 = -53.8429 + 0.117197R_4, \quad (\text{A.4d})$$

$$b_3 = -103.614 + 0.184865R_4. \quad (\text{A.4e})$$

In Figure 19 we have plotted the first positive numerator and denominator zeros of (A.4a) as a function of R_4 , the unknown five-loop term. A positive denominator zero (λ_d) occurs over the entire range of R_4 and precedes the numerator zero (λ_n) when positive, consistent with Figure 2-type dynamics. For the [2|2] case, we find from (2.16) and (A.1) that

$$\beta^{[2|2]}(\lambda) = -\frac{11}{3}\lambda^2 \left[\frac{1 + a_1\lambda + a_2\lambda^2}{1 + b_1\lambda + b_2\lambda^2} \right]; \quad (\text{A.5a})$$

$$a_1 = 24.5902 - 0.0535237R_4 \quad (\text{A.5b})$$

$$a_2 = -47.3211 + 0.0844278R_4, \quad (\text{A.5c})$$

$$b_1 = 21.4993 - 0.0535237R_4, \quad (\text{A.5d})$$

$$b_2 = -128.203 + 0.249865R_4. \quad (\text{A.5e})$$

As is evident from Fig. 20, the first positive numerator zero (λ_n) is always preceded by a positive denominator zero (λ_d), which serves as the infrared-attractor for Figure 2-type dynamics, regardless of the unknown five-loop term R_4 .

Incorporation of a $[3|1]$ approximant within the Padé-summation of (A.1) yields a positive denominator zero only if $R_4 > 0$. This is because $\lambda_d = R_3/R_4$, as is evident from (2.16a) and (2.16e). Hence, if $R_4 < 0$, infrared dynamics along the lines of Fig. 2 are no longer possible. However, we have found that no positive numerator zero exists for this regime, also excluding the possibility of Fig. 1 type dynamics governed by an infrared-stable fixed point. If R_4 is positive, the denominator zero is once again seen to precede all positive numerator zeros, again consistent with Figure 2 type dynamics. All of this behaviour can be extracted from (2.16) and (A.1):

$$\beta^{[3|1]}(\lambda) = -\frac{11}{3}\lambda^2 \frac{[1 + a_1\lambda + a_2\lambda^2 + a_3\lambda^3]}{[1 + b_1\lambda]} \quad (\text{A.6a})$$

$$a_1 = 3.09091 - 0.0116221R_4 \quad (\text{A.6b})$$

$$a_2 = 14.2929 - 0.0359227R_4, \quad (\text{A.6c})$$

$$a_3 = 86.0433 - 0.167698R_4, \quad (\text{A.6d})$$

$$b_1 = -0.0116221R_4. \quad (\text{A.6e})$$

The absence of a positive numerator zero when R_4 is negative necessarily follows from the fact that a_1, a_2 , and a_3 are all positive when $R_4 < 0$.

References

- [1] J. Ellis, I. Jack, D.R.T. Jones, M. Karliner, and M. A. Samuel, Phys. Rev. **D57** (1998), 2665.
- [2] J. Ellis, M. Karliner and M. A. Samuel, Phys. Lett. **B400** (1997), 176.
- [3] V. Elias, T.G. Steele, F.Chishtie, R. Migneron and K. Sprague, Phys. Rev. **D58** (1998), 116007.
- [4] F. Chishtie, V. Elias, T.G. Steele, Phys. Lett. **B466** (1999), 267.
- [5] H. Kleinert, J. Neu, V. Schulte-Frohlinde, K.G. Chetyrkin and S. A. Larin, Phys. Lett. **B272**, 39 (1991); **319** (1993), 545 (E).
- [6] F. Chishtie, V. Elias, T.G. Steele, Phys. Rev. **D59** (1999), 105013.
- [7] A.I. Vainshtein and V.I. Zakharov, Phys. Rev. Lett. **73** (1994), 1207.
- [8] M.A. Samuel, J. Ellis and M. Karliner, Phys. Rev. Lett. **74**, 4380 (1995), 4380.
J. Ellis, E. Gardi, M. Karliner and M. A. Samuel, Phys. Lett. **B366** (1996), 268 .
- [9] E. Gardi, Phys. Rev. **D56** (1997), 68.
- [10] I.I. Kogan and M. Shifman, Phys. Rev. Lett. **75** (1995), 2085.
- [11] A.C. Mattingly and P.M. Stevenson, Phys. Rev. Lett. **69**(1992), 1320.
P.M. Stevenson, Phys. Lett. **B331** (1994), 187.
- [12] A.C. Mattingly and P. M. Stevenson. Phys. Rev. **D49** (1994), 437.
- [13] T. Appelquist, J. Terning and L.C.R. Wijewardhana, Phys. Rev. Lett. **77** (1996), 1214.
T. Appelquist, A. Ratnaweera, J. Terning and L.C.R. Wijewardhana, Phys. Rev. **D58**(1998), 105017.
T. Appelquist and F. Sannino, Phys. Rev. **D59** (1999), 067702.
- [14] V. A. Miransky and K. Yamawaki, Phys. Rev. **D55** (1997), 5051 and Erratum **56** (1997), 3768.
V. A. Miransky, Phys. Rev. **D59** (1999), 105003.
- [15] R. S. Chivukula, Phys. Rev. **D55** (1997), 5238.
- [16] M. Velkovsky and E. Shuryak, Phys. Lett. **B437** (1998), 398.
- [17] E. Gardi and M. Karliner, Nucl. Phys. **B529** (1998), 383.
E. Gardi, G. Grunberg and M. Karliner, JHEP **07** (1998), 007.
E. Gardi and G. Grunberg, JHEP **9903** (1999), 024.
- [18] T. Banks and A. Zaks, Nucl. Phys. **B196** (1982), 189.
- [19] T. van Ritbergen, J.A. M. Vermaseren and S.A. Larin, Phys. Lett. **B405** (1997), 323.
- [20] G. 't Hooft, Nucl. Phys. **B72** (1974), 461.
- [21] V. Novikov, M. Shifman, A. Vainshtein and V. Zakharov, Nucl. Phys. **B229** (1983), 381, and Phys. Lett. **B166** (1986), 329.
- [22] D.R.T. Jones, Phys. Lett. **B123** (1983), 45.
- [23] M. J. Teper, Phys. Rev. **D59** (1999), 014512.
C. Morningstar and M. Peardon, Phys. Rev. **D56** (1997), 4043 and Phys. Rev. **D60** (1999), 03459.
M. Peardon, Nucl. Phys. B (Proc. Suppl.) **63** (1999), 22.
- [24] C. Csáki, H. Ooguri, Y. Oz, and J. Terning, JHEP **9901** (1999), 017. R. de Mello Koch, A. Jevicki, M. Mihailescu, and J. Nunes, Phys. Rev. **D58** (1998), 105009.
M. Zyskin, Phys. Lett. **B439** (1998), 373.

- [25] J. Maldacena, Adv. Theor. Math. Phys. **2** (1998), 231.
E. Witten, Adv. Theor. Math. Phys. **2** (1998), 505.
- [26] P. I. Fomin, V. P. Gusynin, V. A. Miransky and Yu. A. Sitenko, Riv. Nuovo Cim. **6** (1983), 1.
K. Higashijima, Prog. Theor. Phys. Suppl. **104** (1991), 1.
V. A. Miransky, *Dynamical Symmetry Breaking in Quantum Field Theories* (World Scientific, Singapore, 1993).
C. D. Roberts and A.G. Williams, Prog. Part. Nucl. Phys. **33** (1994), 477.
- [27] Y. Iwasaki, K. Kanaya, S. Sakai, T. Yoshié, Phys. Rev. Lett. **69** (1992), 21.
- [28] C. Caso et. al. [Particle Data Group], Eur. Phys. J. C **3** (1998), 1.
- [29] G. 't Hooft, “Can we make sense out of Quantum Chromodynamics?”, in *The Whys of Subnuclear Physics: Erice 1977*, A. Zichichi, ed. (Plenum, New York, 1979).

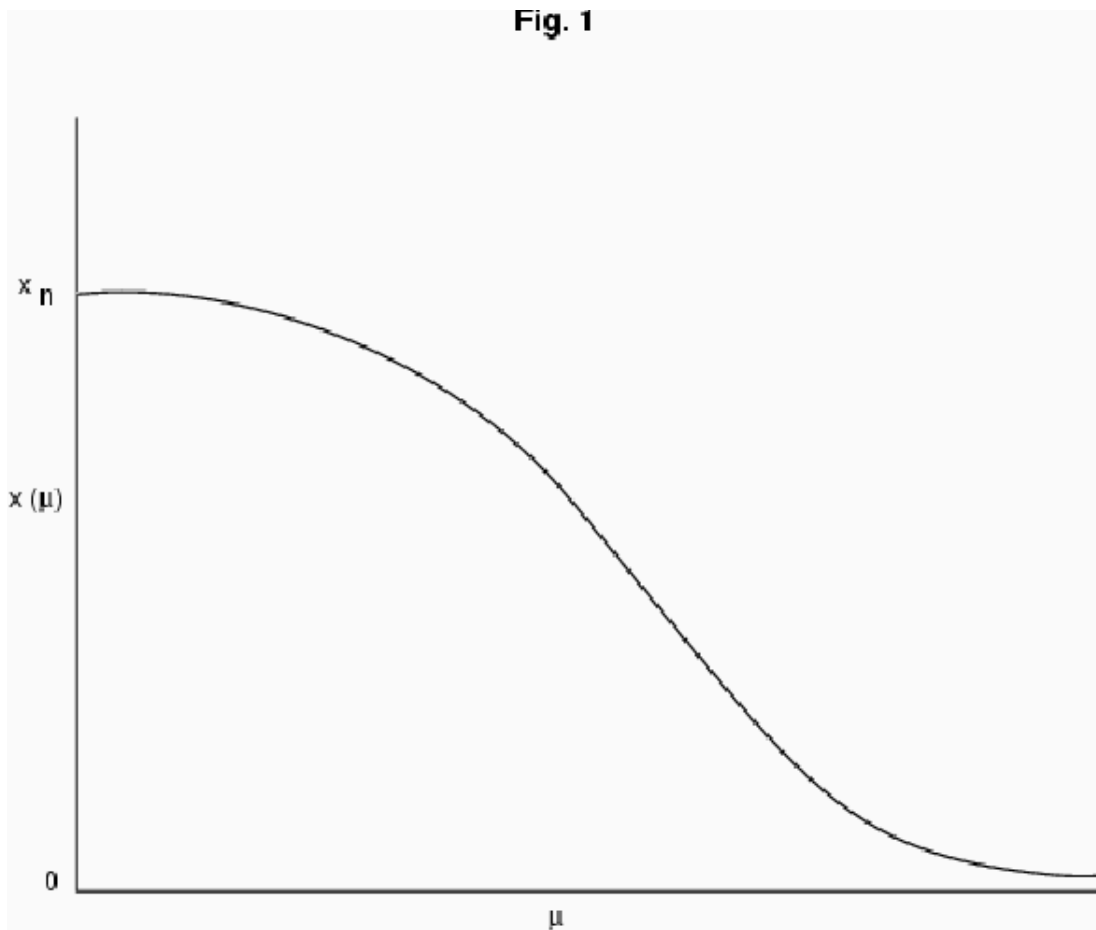


Figure 1: Behaviour of the asymptotically-free running couplant $x(\mu) \equiv \alpha_s(\mu)/\pi$ in dynamics governed by an infrared-stable fixed point x_n .

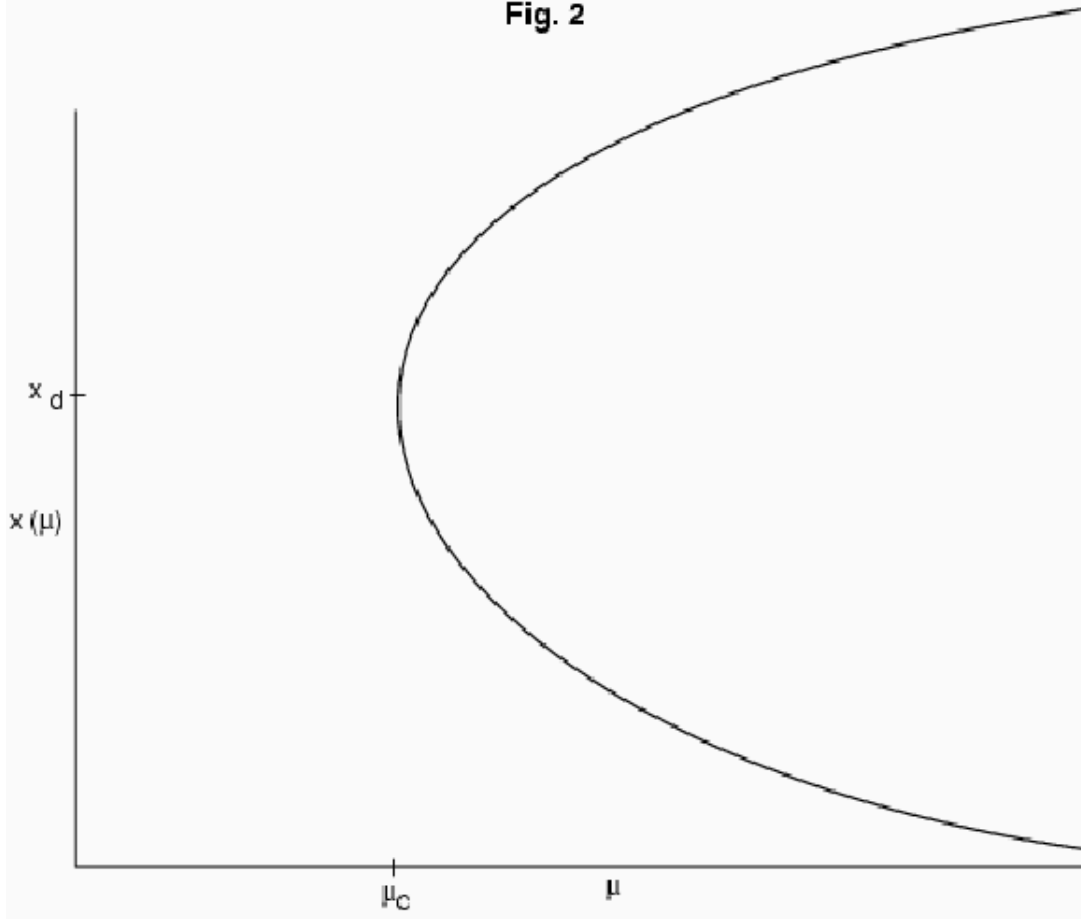


Figure 2: Behaviour of the asymptotically-free running couplant $x(\mu)$ in dynamics governed by a β -function pole at x_d . The point x_d serves as an infrared attractor of both a strong and weak phase of the couplant. An infrared cut-off μ_c necessarily occurs, corresponding to the β -function pole at $x(\mu_c) = x_d$.

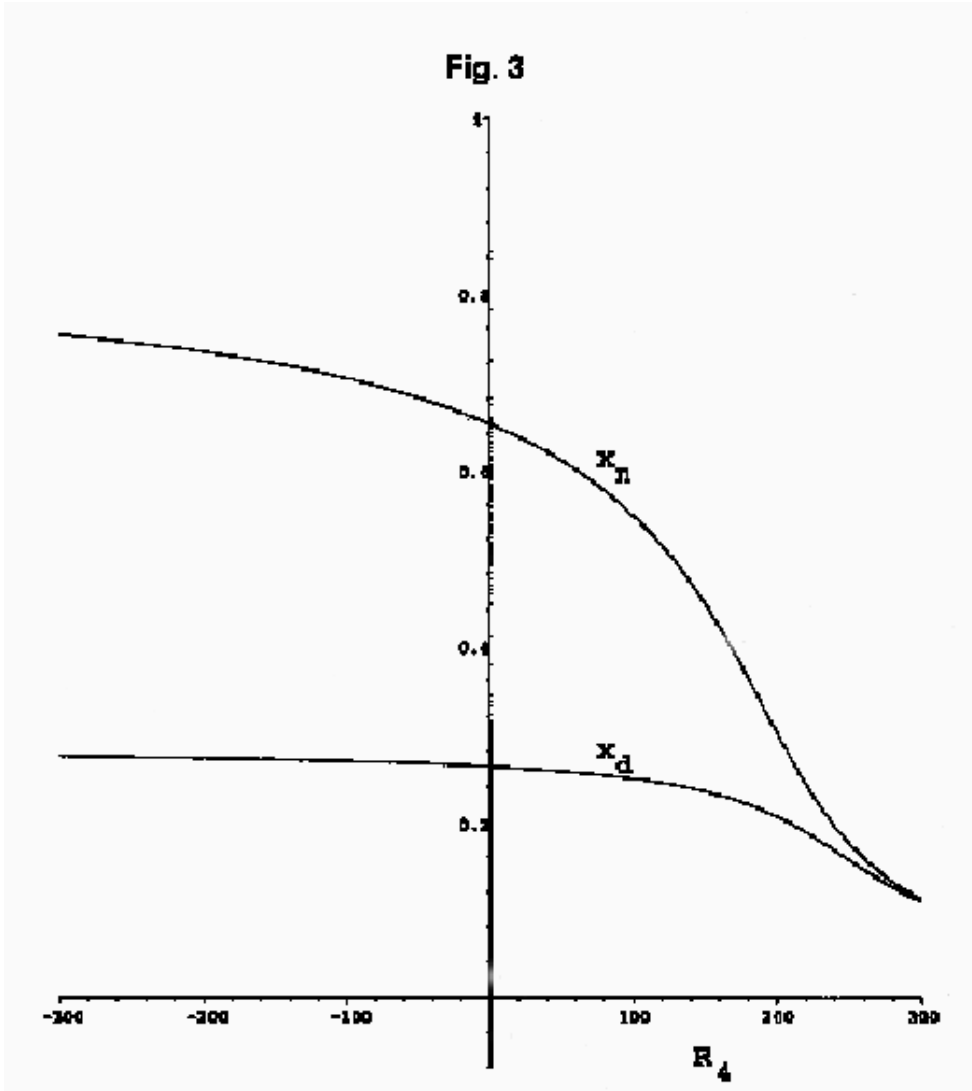


Figure 3: The R_4 -dependence of the first positive numerator zero (x_n) and the first positive denominator zero (x_d) of the $[2|2]$ Padé-summation of the QCD β -function when $n_f = 0$. The independent variable $R_4 \equiv \beta_4/\beta_0$ is proportional to the presently unknown 5-loop contribution (β_4) to the β -function. The figure shows that x_d and x_n both exist over the entire range of R_4 . However, x_d always precedes x_n , indicative of the dynamics of Figure 2 for the evolution of the couplant $x(\mu)$ from the asymptotically-free ultraviolet region.

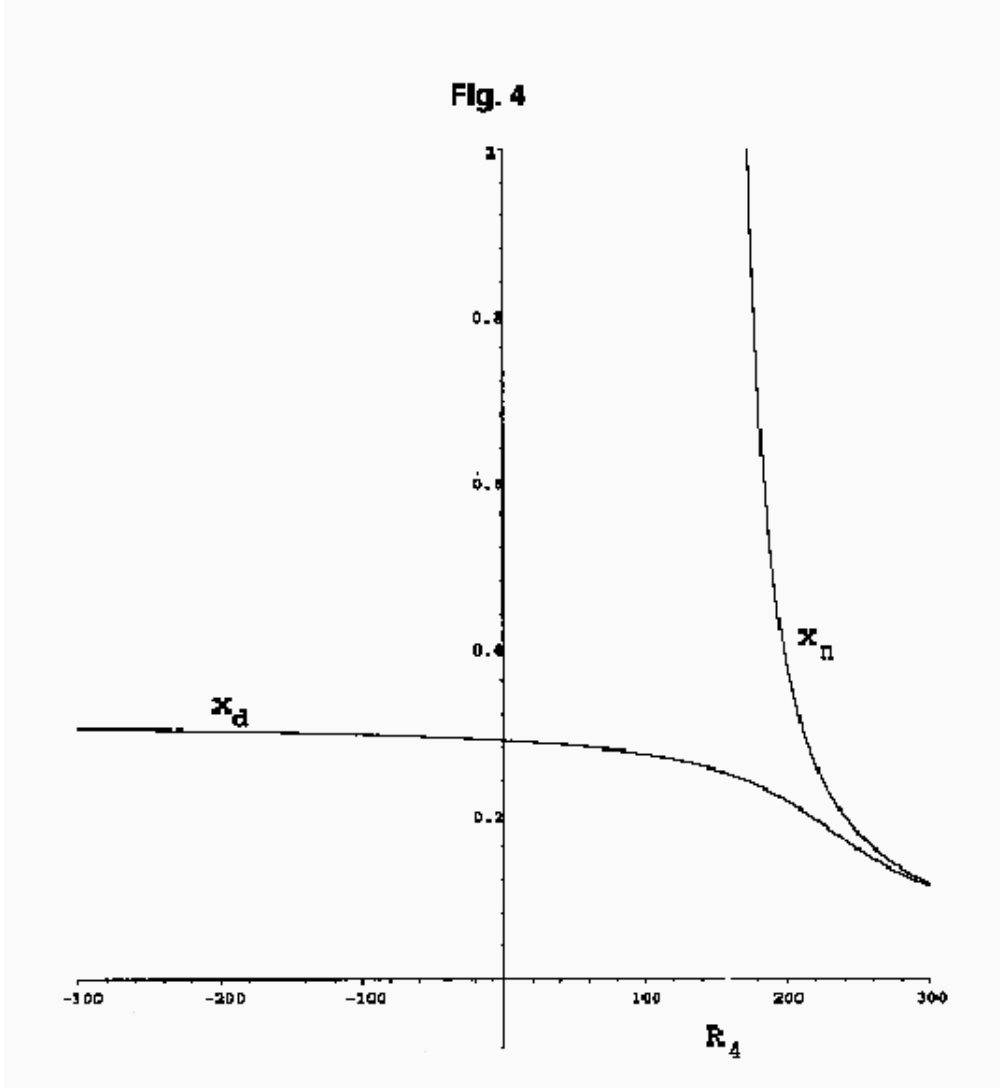


Figure 4: The R_4 -dependence [$R_4 \equiv \beta_4/\beta_0$] of the first positive numerator zero (x_n) and the first positive denominator zero (x_d) of the $[1/3]$ Padé-summation of the QCD β -function when $n_f = 0$. The figure shows that x_d exists over the entire range of R_4 . Moreover, x_d precedes x_n over the range of R_4 for which a positive numerator zero exists, leading once again to the dynamics of Figure 2 for the evolution of the couplant from the asymptotically-free ultraviolet region.

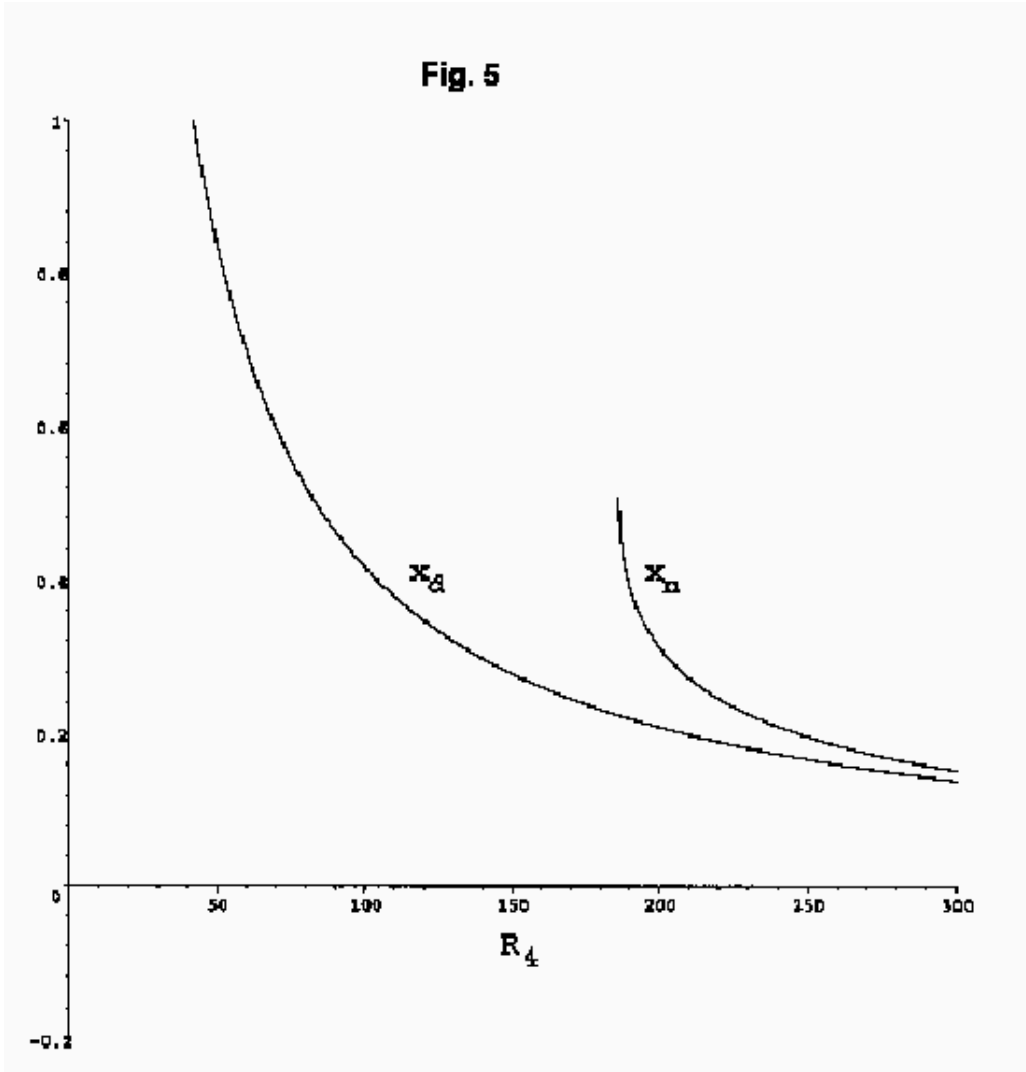


Figure 5: The R_4 -dependence [$R_4 \equiv \beta_4/\beta_0$] of the first positive numerator zero (x_n) and the first positive denominator zero (x_d) of the [3|1] Padé-summation of the QCD β -function when $n_f = 0$. As in Figures 3 and 4, x_d exists over the entire range of R_4 , and x_d precedes x_n where a positive numerator zero exists.

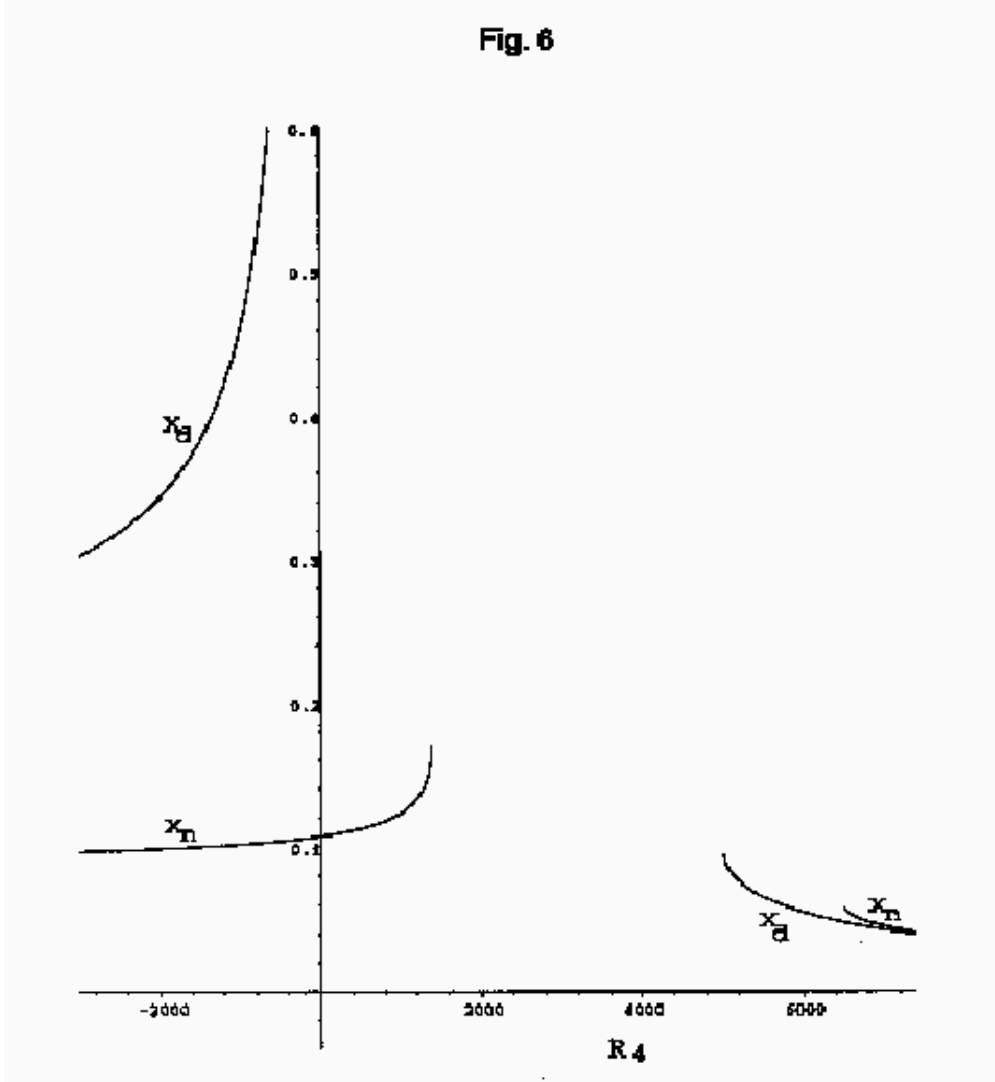


Figure 6: The behaviour over a very large region of R_4 of the first positive numerator zero (x_n) and the first positive denominator zero (x_d) of the $[2|2]$ Padé-summation of the QCD β -function when $n_f = 13$. The figure shows that x_n precedes x_d when $R_4 < 1383$, indicative of dynamics governed by an infrared-stable fixed point (Figure 1) for this region. The figure also shows that x_d precedes x_n when R_4 is very large ($R_4 > 5020$), indicative of dynamics governed by a β -function pole (Figure 2). The absence of a positive β -function zero for R_4 between 1383 and 5020 precludes the possibility of dynamics governed by an infrared-stable fixed point for this range of R_4 .

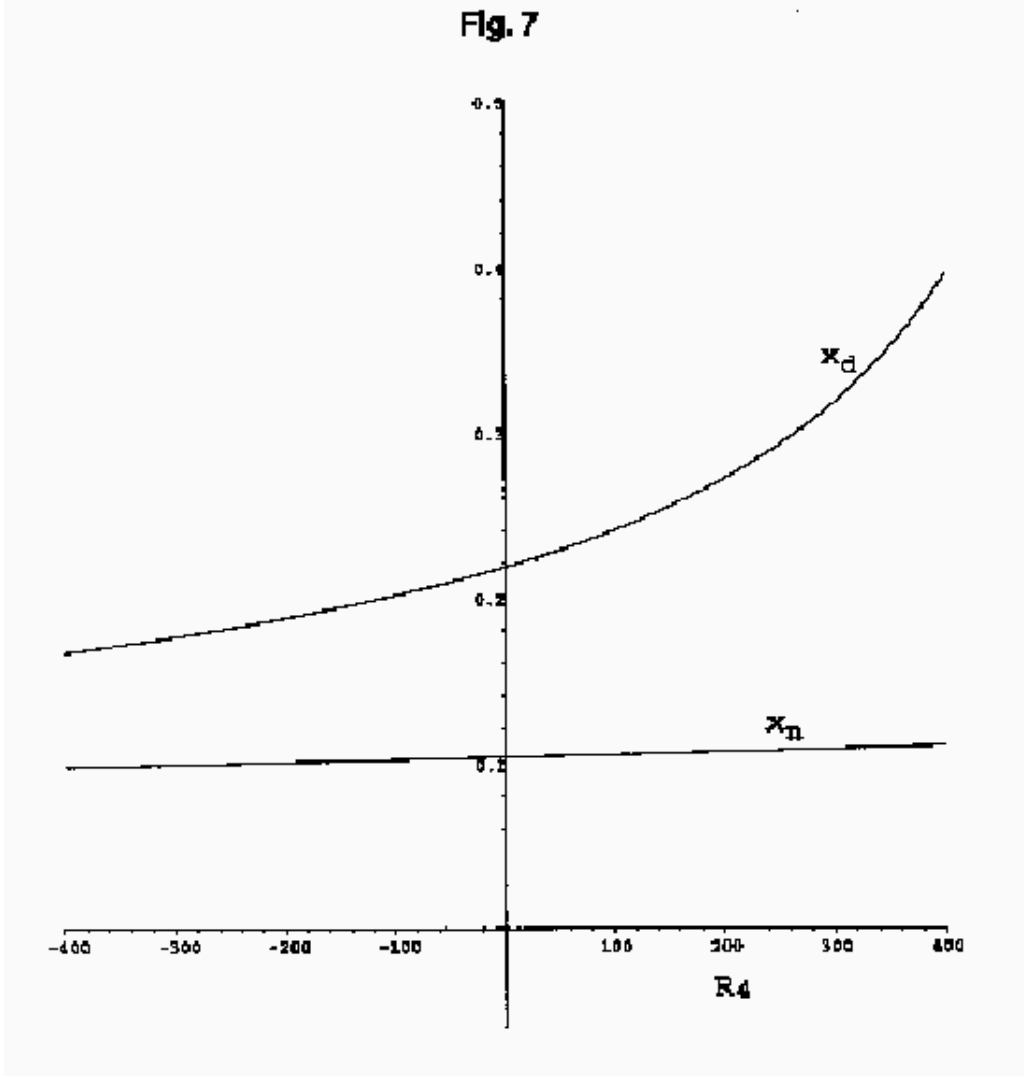


Figure 7: The R_4 -dependence of the first positive numerator zero (x_n) and the first positive denominator zero (x_d) of the $[1|3]$ Padé-summation of the QCD β -function when $n_f = 13$. The numerator zero is seen to precede the denominator zero over the entire range of R_4 exhibited, consistent with the numerator zero serving as an infrared-stable fixed point. This numerator zero ceases to be positive when $R_4 > 6394$.

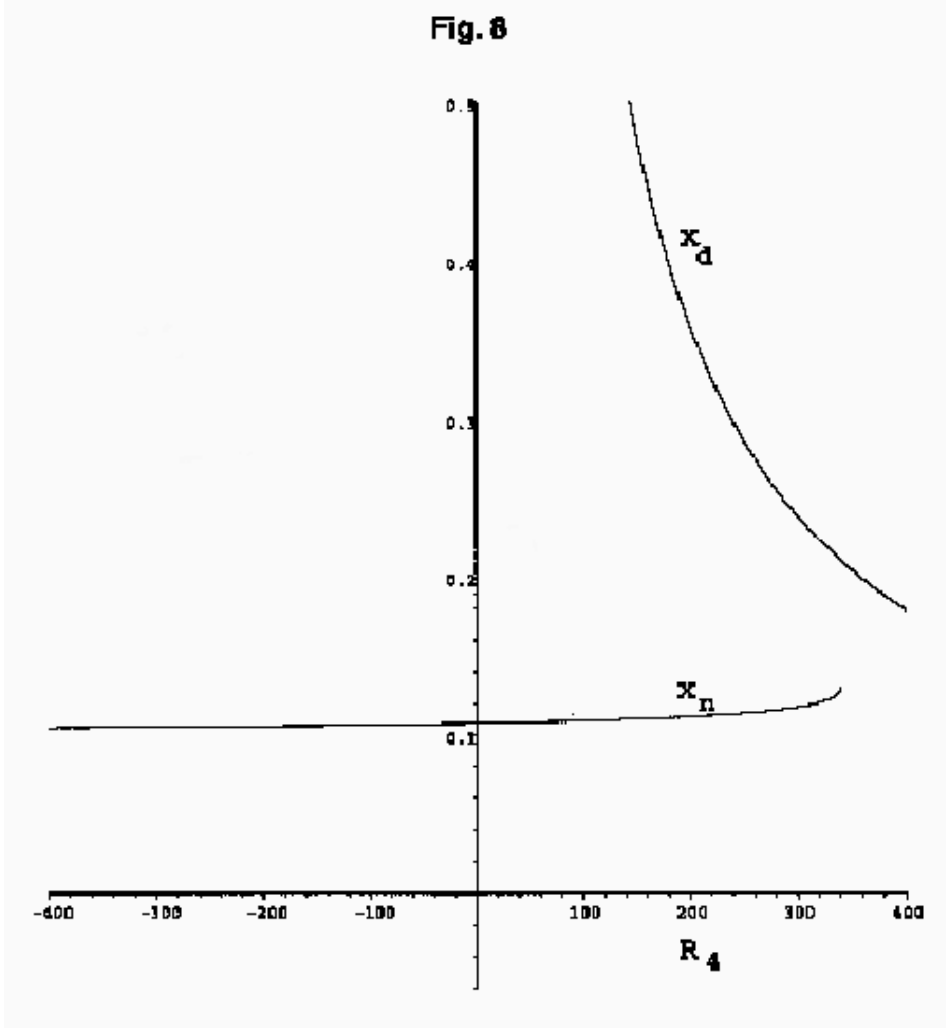


Figure 8: The R_4 -dependence of the first positive numerator zero (x_n) and the first positive denominator zero (x_d) of the [3|1] Padé-summation of the QCD β -function when $n_f = 13$. The numerator zero is seen to precede the denominator zero when $R_4 < 340$, corresponding to the domain of R_4 for dynamics governed by the infrared-stable fixed point x_n . The denominator zero precedes any positive numerator zeros that occur for $R_4 > 340$, corresponding to Figure 2 dynamics governed by an infrared attractor at x_d .

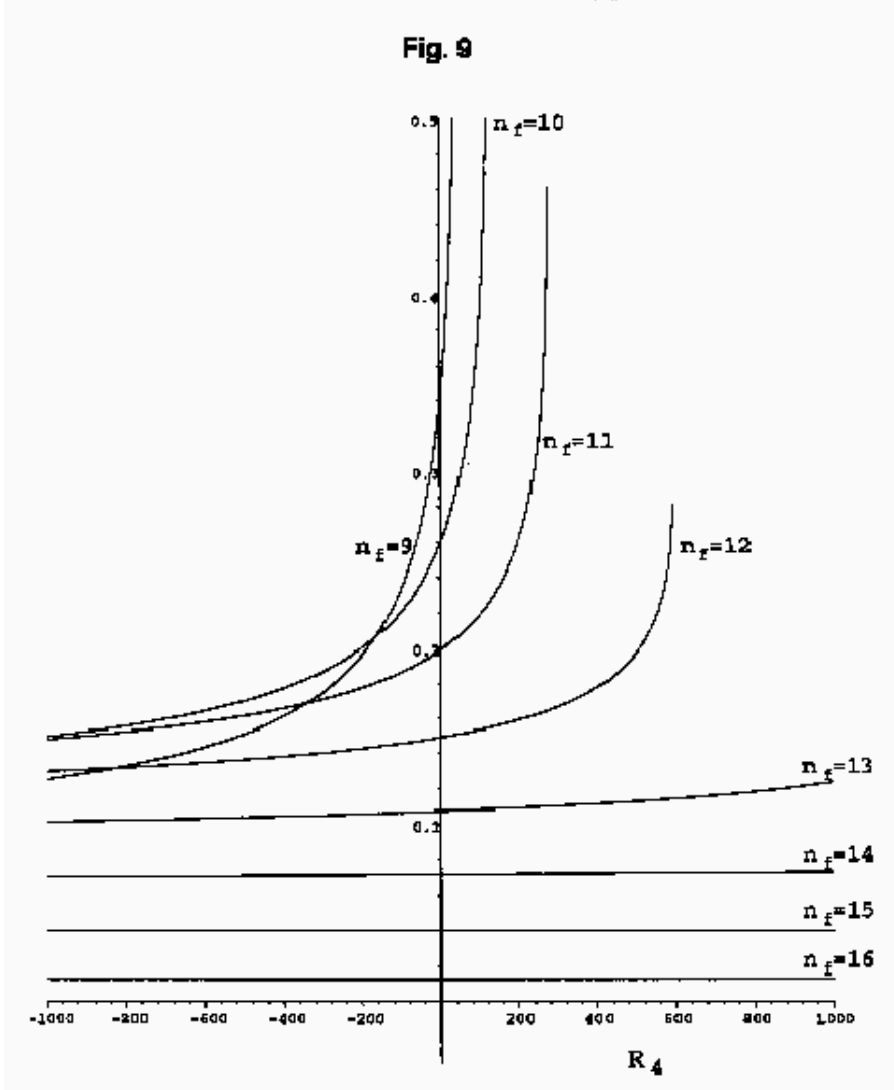


Figure 9: The n_f -dependence of the infrared fixed point x_n , as indicated by successive plots of x_n versus R_4 for $\beta^{[2|2]}$ with values of n_f ranging from 9-16.

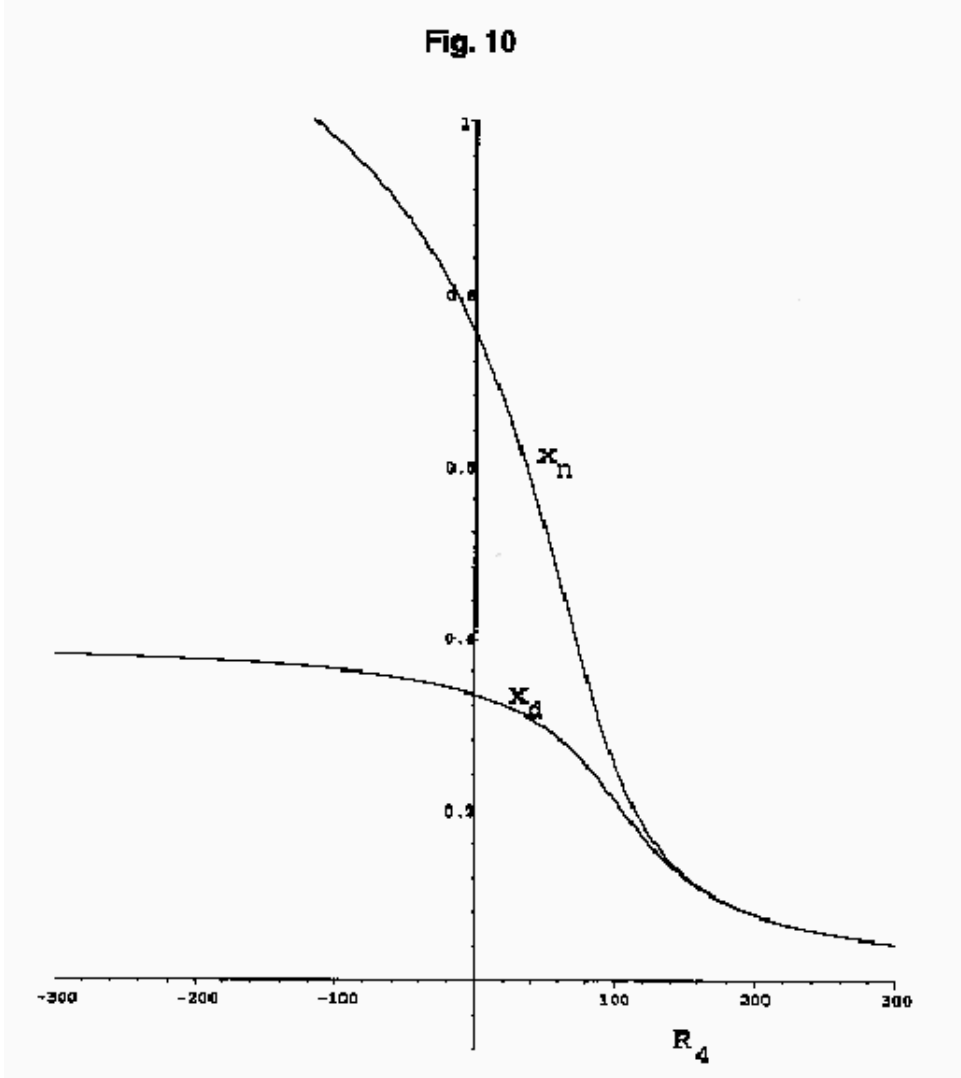


Figure 10: The R_4 -dependence of the first positive numerator zero (x_n) and the first positive denominator zero (x_d) of the $[2|2]$ Padé-summation of the QCD β -function when $n_f = 3$. The figure shows that x_d always precedes x_n , indicative of infrared-attractor dynamics (Figure 2).

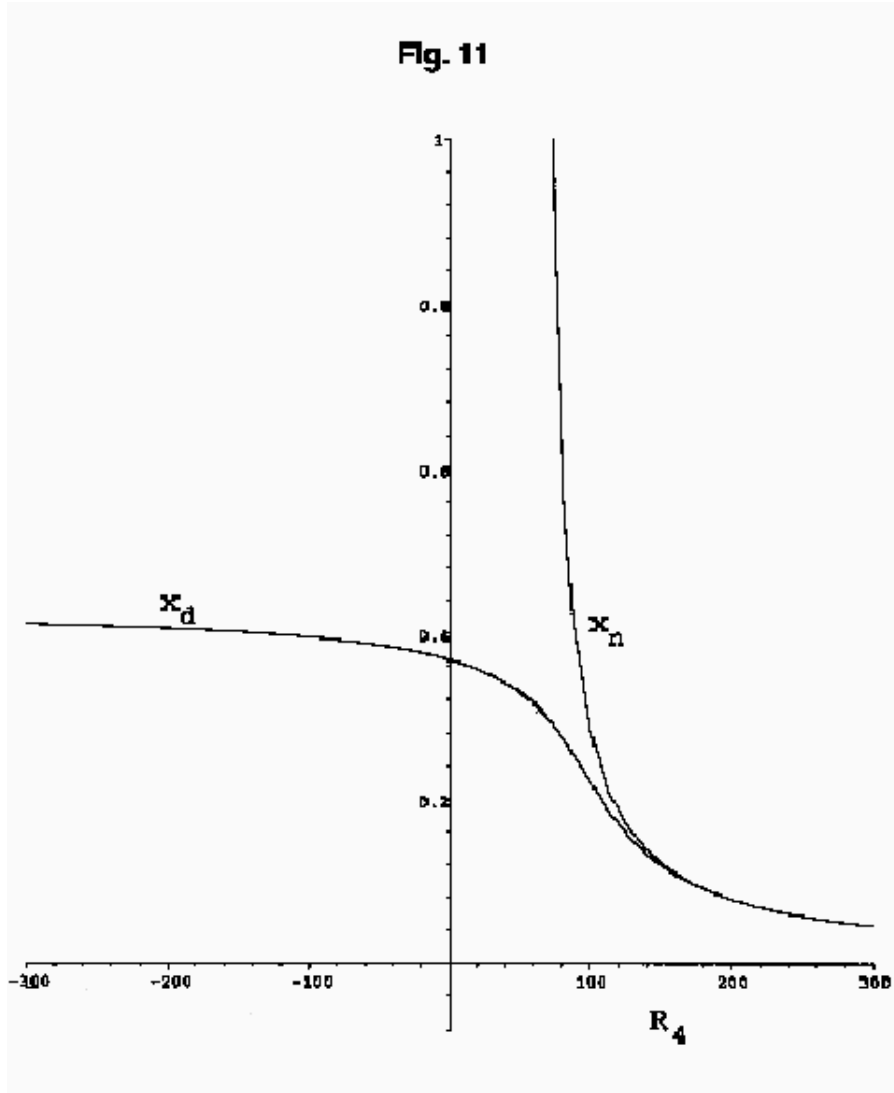


Figure 11: The R_4 -dependence of the first positive numerator zero (x_n) and the first positive denominator zero (x_d) of the $[1|3]$ Padé-summation of the QCD β -function when $n_f = 3$. The figure shows that x_d exists over the entire range of R_4 , and precedes x_n over the range where such a positive zero exists. Hence x_d serves as an infrared attractor.

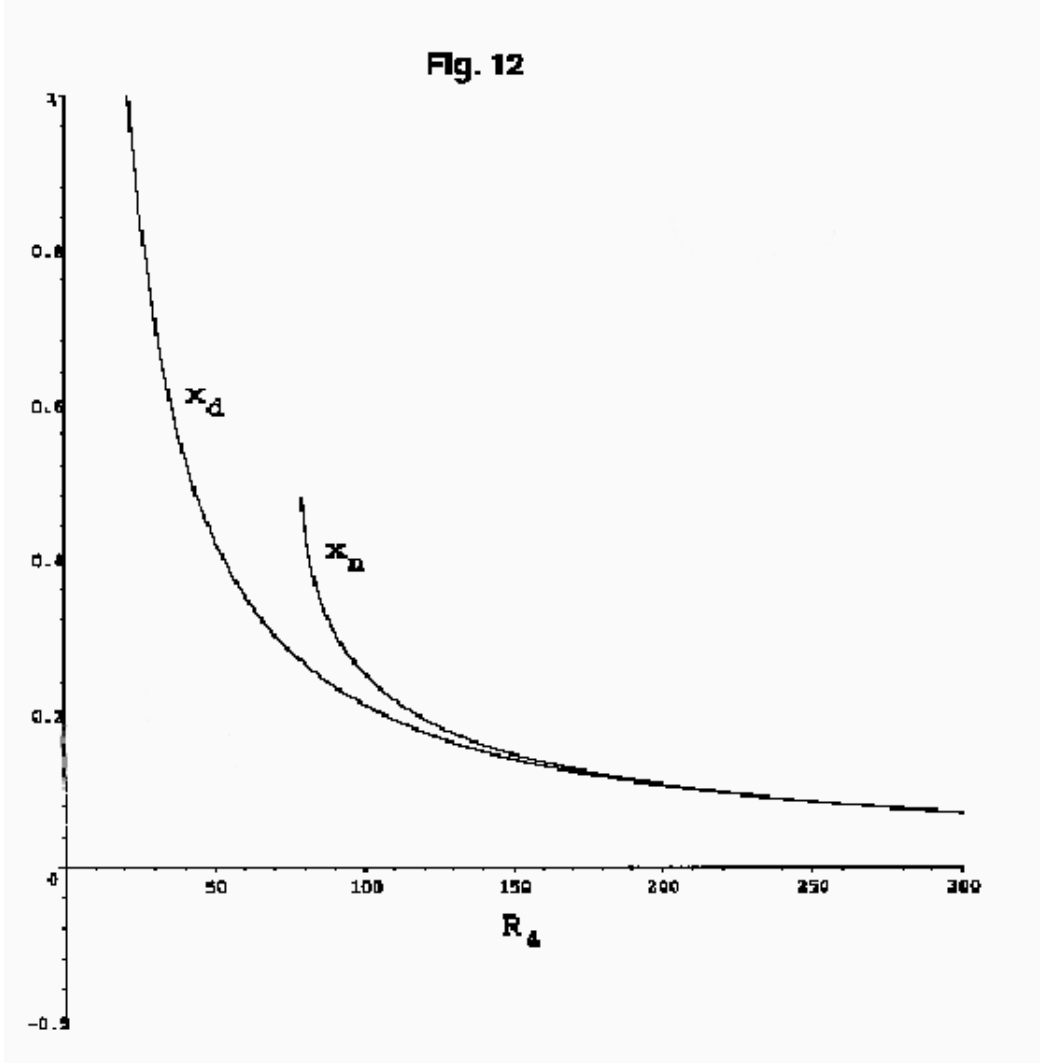


Figure 12: The R_4 -dependence of the first positive numerator zero (x_n) and the first positive denominator zero (x_d) of the $[3|1]$ Padé-summation of the QCD β -function when $n_f = 3$. The figure shows that x_d exists over the entire range of R_4 , and precedes x_n over the range where such a positive zero exists, as in Fig. 11. Hence x_d serves as an infrared attractor for this case as well.

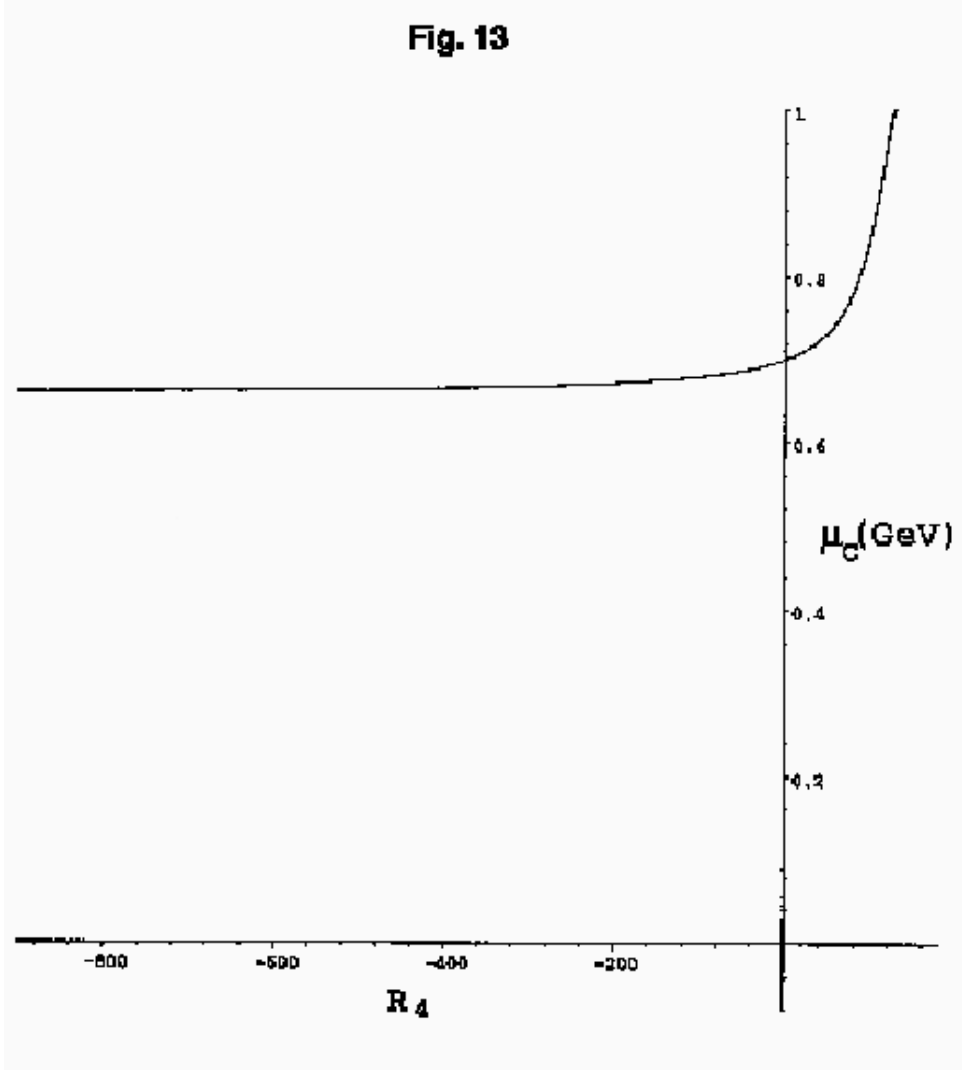


Figure 13: The R_4 -dependence of μ_c , the minimum value of μ accessible to the couplant $x(\mu)$ derived from $\beta^{[2|2]}$ when $n_f = 3$. The 1 GeV value of the couplant is assumed to be $x(1) = 0.153$, as discussed in the text

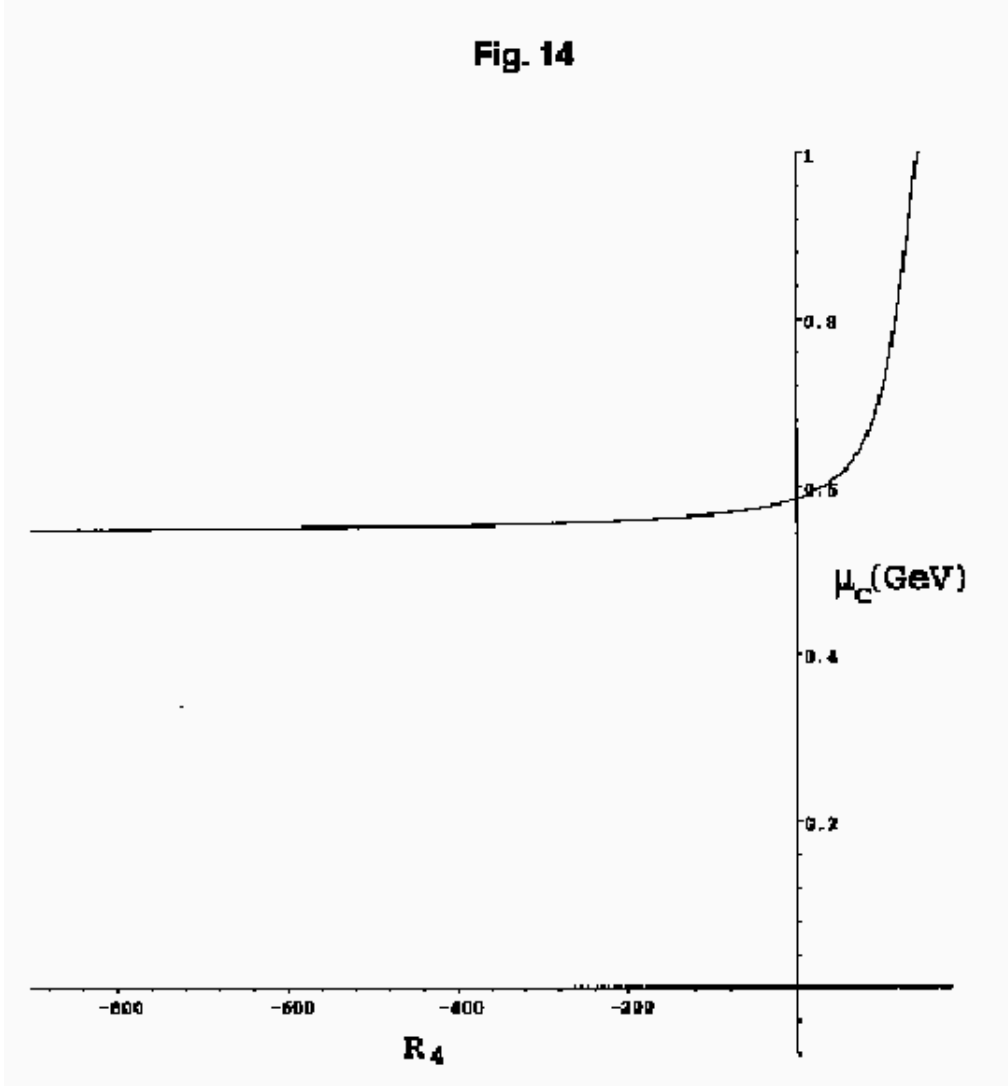


Figure 14: The R_4 -dependence of μ_c , as in Figure 13, except that the 1 GeV value of the couplant is given a lower-bound value $x(1) = 0.1305$.

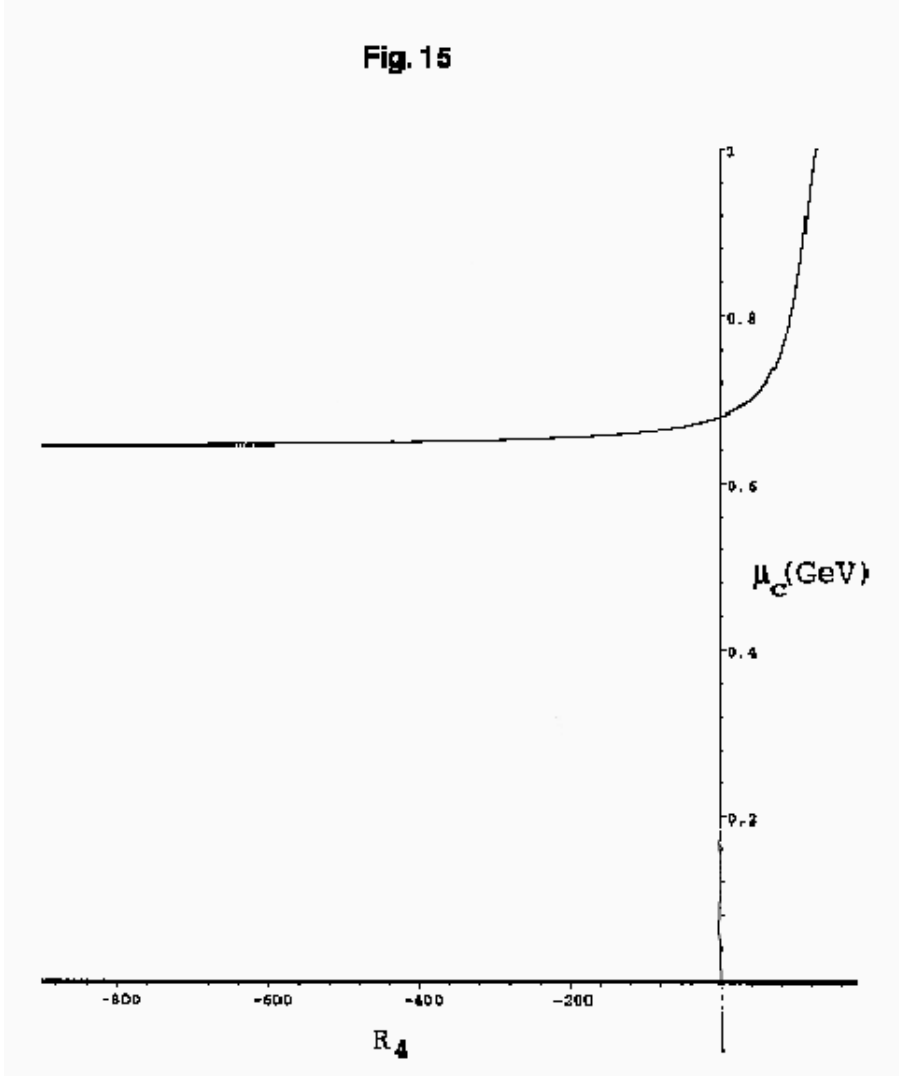


Figure 15: The R_4 -dependence of μ_c , the minimum value of μ accessible to the couplant $x(\mu)$ derived from $\beta^{[1|3]}$ when $n_f = 3$ and $x(1) = 0.153$.

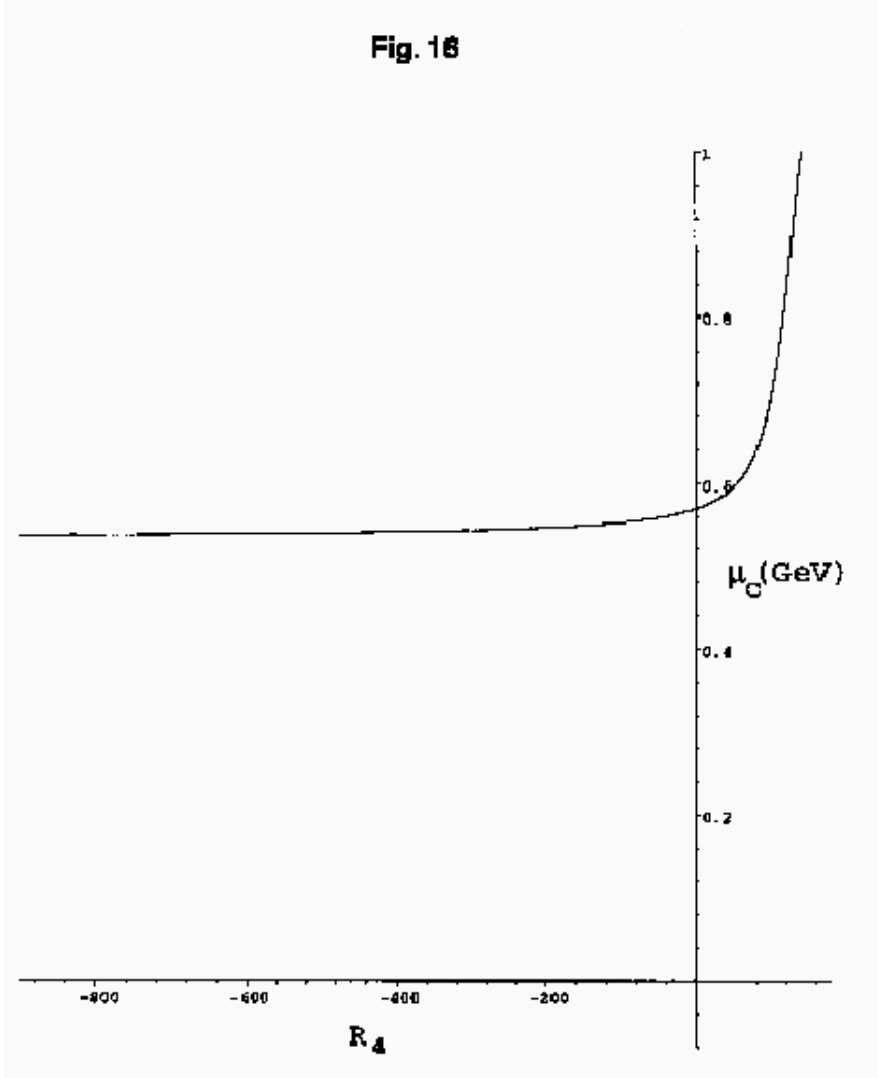


Figure 16: The R_4 -dependence of μ_c , as in Figure 15, except that the 1 GeV value of the couplant is given a lower-bound value $x(1) = 0.1305$.

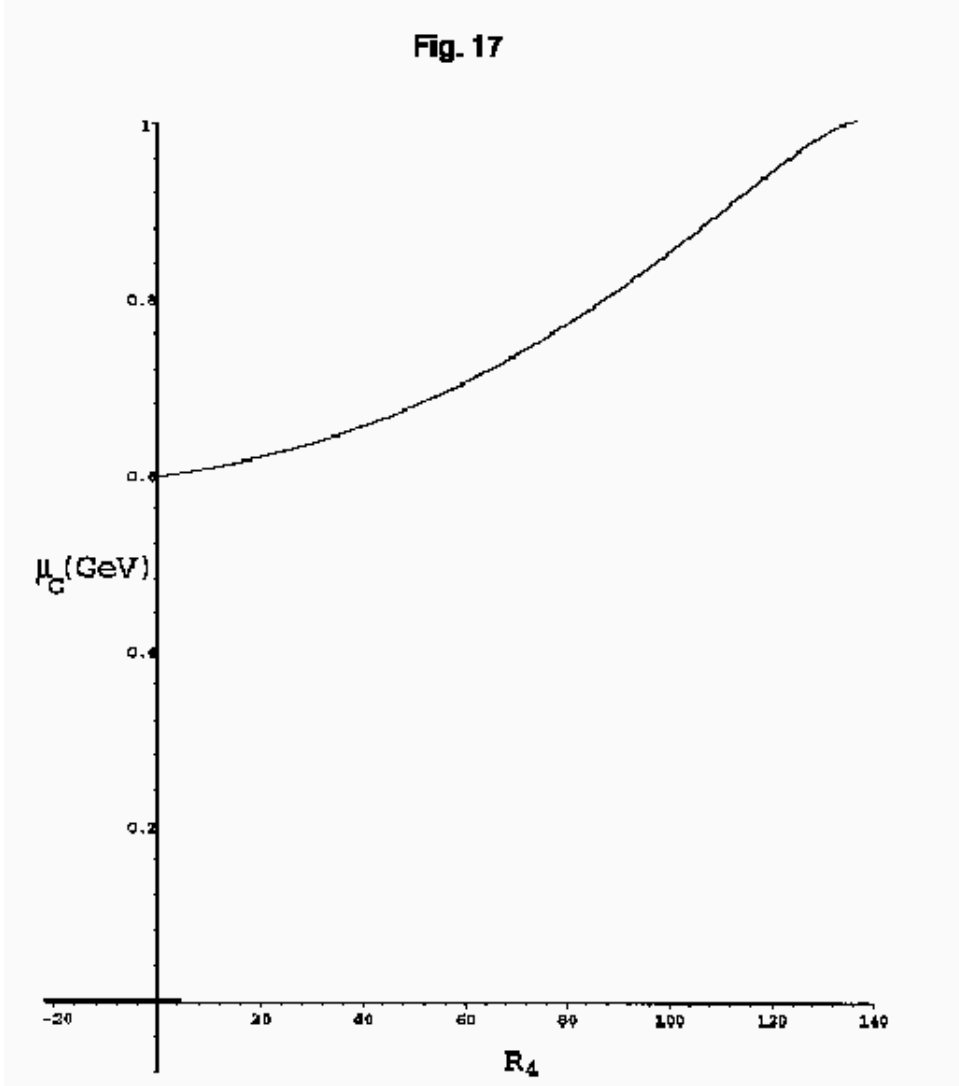


Figure 17: The R_4 -dependence of μ_c , the minimum value of μ accessible to the couplant $x(\mu)$ derived from $\beta^{[3|1]}$ when $n_f = 3$ and $x(1) = 0.153$. The couplant has an infrared attractor for this case only if R_4 is positive.

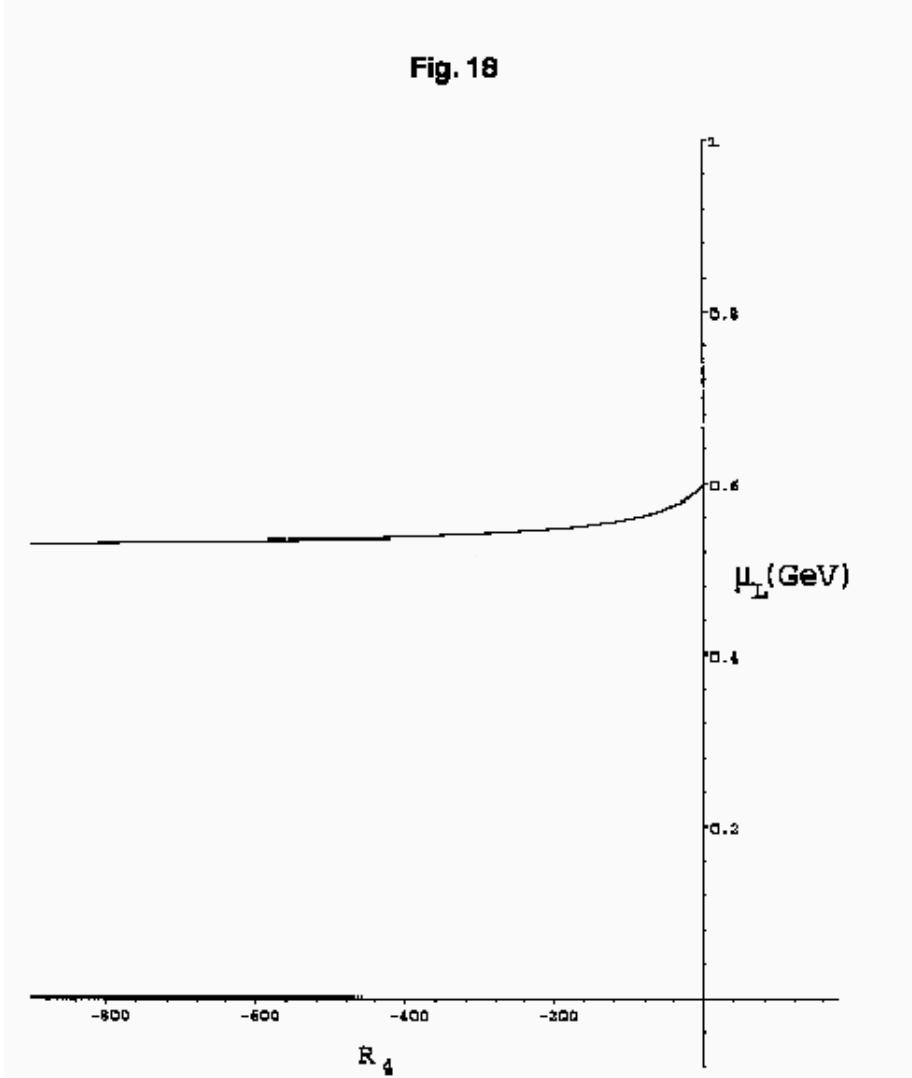


Figure 18: The R_4 -dependence of the Landau pole μ_L of the couplant derived from $\beta^{[3|1]}$ when $n_f = 3$ and $x(1) = 0.153$. This Landau pole (as opposed to an infrared attractor of two ultraviolet phases) occurs only for negative values of R_4 .

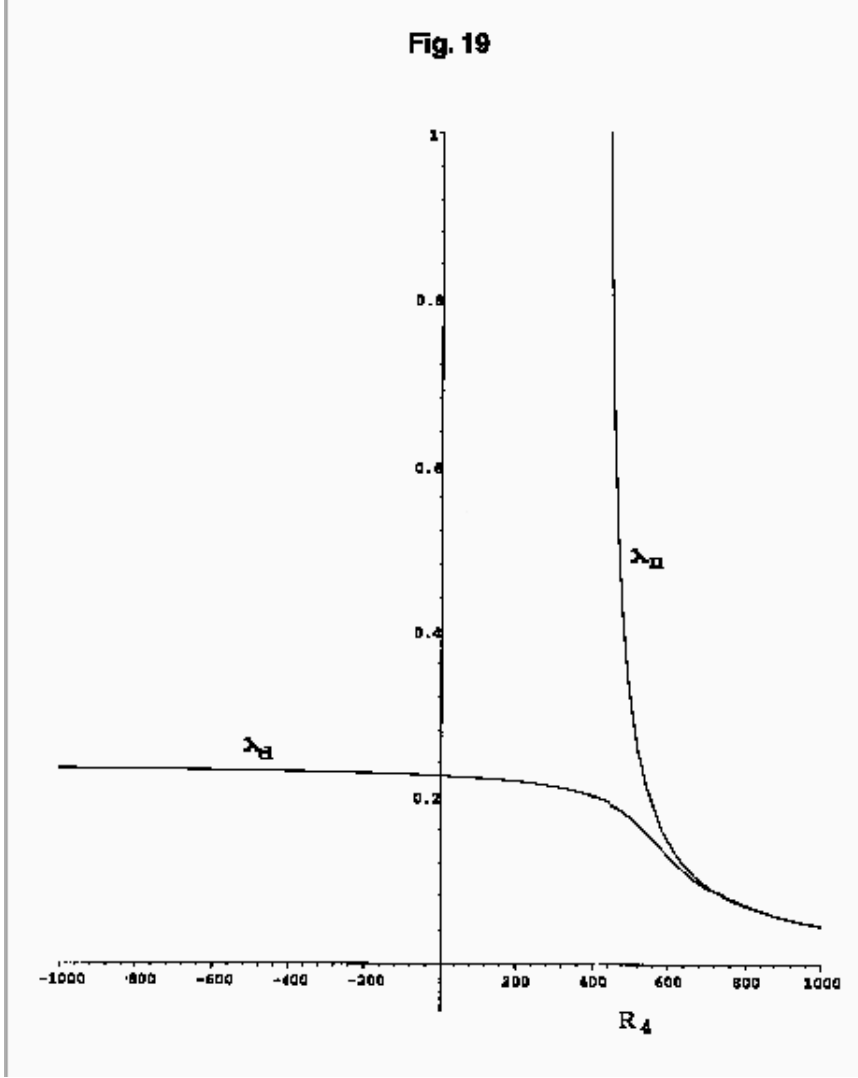


Figure 19: The dependence on the unknown five-loop term R_4 of the first positive numerator zero (λ_n) and the first positive denominator zero (λ_d) of the [1|3] Padé-summation of the $SU(N_c)$ β -function for the couplant $\lambda = N_c \alpha(\mu)/4\pi$ in the $N_c \rightarrow \infty$ limit ($n_f = 0$). The figure shows that the denominator zero λ_d exists over the range of R_4 and precedes the first positive numerator zero λ_n when such a zero exists, indicative of Figure 2 dynamics with λ_d serving as the infrared attractor.

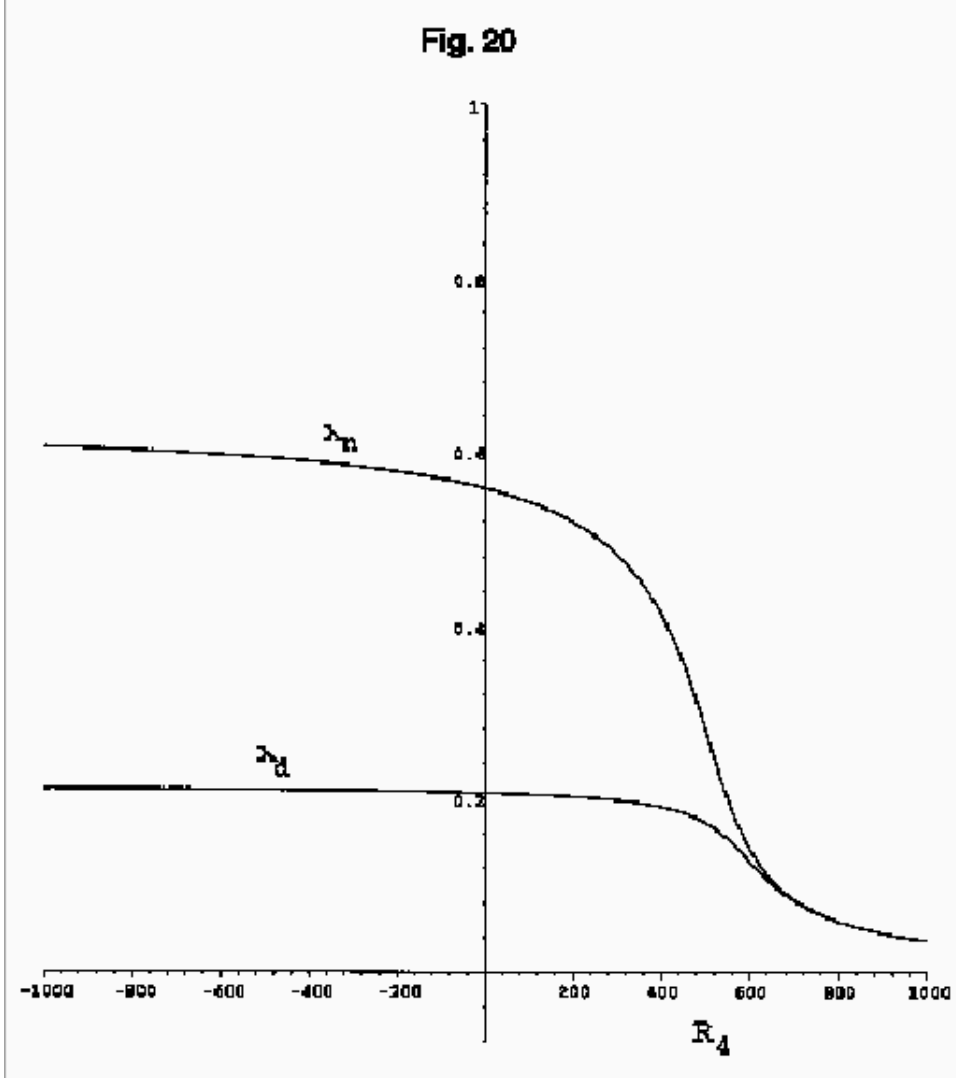


Figure 20: The R_4 -dependence of the first positive numerator zero (λ_n) and the first positive denominator zero (λ_d) of the [2|2] Padé-summation of the $SU(N_c)$ β -function for the couplant $\lambda = N_c \alpha(\mu)/4\pi$ in the $N_c \rightarrow \infty$ limit ($n_f = 0$). Once again, the denominator zero λ_d exists over the entire range of R_4 and precedes the first positive numerator zero λ_n .